A STUDY ON MICRO-PATTERNING OF POLYPYRROLE USING MICRO-ELECTRO-DISCHARGE MACHINING

by

Mohammed Muntakim Anwar

M.Eng., National University of Singapore, 2008

B.Sc., Bangladesh University of Engineering and Technology, 2004

A THESIS SUBMITTED IN PARTIAL FULFILLMENT OF
THE REQUIREMENTS FOR THE DEGREE OF

MASTER OF APPLIED SCIENCE

in

THE FACULTY OF GRADUATE STUDIES

(Electrical and Computer Engineering)

THE UNIVERSITY OF BRITISH COLUMBIA
(Vancouver)

October 2012

Abstract

This thesis reports micro-patterning of polypyrrole based on micro-electro-discharge machining (μEDM). The patterning feasibility is investigated using air and EDM oil as the dielectric media for the process. The discharge generation and controlled removal of the material are observed in both dielectric media; however, processing in oil is shown to be superior in achieving higher machining quality. The use of a discharge voltage of 60 V without an external capacitor as part of the relaxation-type discharge circuit is found to enable stable and precision machining with 51 nm average surface roughness and 18 mA peak discharge current. Fine micro-patterning of polypyrrole film for a depth of 7.5 μm is demonstrated using a 20-μm-diameter electrode. Machining tests with varying voltages and capacitances indicates that the use of larger capacitances at 60 V does not enhance EDM removal much unlike typical μEDM of metals, whereas the use of larger voltages with stray capacitance shows significant enhancement; a hypothesis to explain these observations is proposed. Scaling effects in machining precision and surface quality are revealed to show that the use of smaller electrodes for smaller structure patterning provides higher structural integrity and smoother and/or cleaner surfaces, an advantageous feature as a micro-machining technique for this material. The generated discharge pulses were measured to exhibit a peak current of 37 mA and a pulse frequency of 0.83 MHz on average. The dependence of electrical contact to polypyrrole samples on the discharge current is evaluated from experiments and simulations. The effects of single spark discharges on polypyrrole and stainless steel were also analyzed. Energy dispersive X-ray was used to analyze the composition of polypyrrole before and after submerging to EDM oil. The results suggested that EDM (and its oil) does not alter composition to a great extent. This study also demonstrates application of μEDM to pattern polypyrrole deposited on catheter to create electrodes. The

actuation of patterned catheter was also verified. The results suggest that μEDM is a promising micro-patterning technique for polypyrrole that will promote micro-device applications for the material and encourage extensions of the study to patterning of other conducting polymers.

Preface

Growth of polypyrrole film on glassy carbon crucible was performed by Lucy Li of Molecular Mechatronics (MM) Lab of UBC supervised by Dr. John D. Madden. Catheter samples were also provided by Molecular Mechatronics Lab. The deposition of polypyrrole on catheter and the experiments of catheter actuation were conducted with help of Umair Naseem Rana of Molecular Mechatronics Lab. LT Spice Simulation were conducted with assistance of Mirza Saquib Us Sarwar of Takahata Lab. I have conducted all other experiments and analysis in accordance with the suggestions of my thesis supervisor, Dr. Kenichi Takahata.

Table of Contents

List of Tables

List of Figures

Acknowledgements

I would like to express my deepest and heartfelt gratitude and appreciation to my supervisor, Dr. Kenichi Takahata for his valuable guidance, continuous support and encouragement throughout my time at UBC. He has provided valuable suggestions from the development of my thesis concept to the fulfillment of my research work. Without his continuous supervision it would have been impossible to manage the research within this short period.

I would like to take this opportunity to show my gratitude Dr. John D. Madden for providing me valuable guidance with research direction and analysis. I would also like thank University of British Columbia (UBC) for providing research facilities. The rich state of the art facilities and support of Takahata Lab, Molecular Mechatronics (MM) Lab, Electron Microscope Laboratory at Materials Engineering and AMPEL Nanofabrication Facility (ANF) provided the opportunity to carry out experiments and their analysis smoothly. I would also like to express my appreciation to Natural Sciences and Engineering Research Council of Canada, the Canada Foundation for Innovation and the British Columbia Knowledge Development fund for financially supporting the research work.

I also would like to take this opportunity to thank the following staff for their sincere help, guidance and advice without which this project would not be successfully completed: Mr Umair Naseem Rana and Ms Lucy Li from Molecular Mechatronics Lab, Mr. Jacob Kabel from Electron Microscope Laboratory and Ms. Alina Kulpa of AMPEL Nanofabrication Facility. Special thanks go to Mr Tanveer Saleh, a postdoctoral fellow of Takahata Lab for his advice during experiments and Masoud Dahmardeh and Babak Assadsanghabi, PhD students of Takahata Lab, for their help with different instrumentation of AMPEL Nanofabrication Facility

for result analysis. I would also like to thank Mr. Mirza Saquib Us Sarwar, a MASc candidate of Takahata Lab, for his valuable advice and encouragement during my work.

I would like to offer my appreciation for the support and encouragement during various stages of this research work to my labmates and friends. My appreciation goes to Anas Amjad Mohammad Bsoul, Reza Rashidi, Mohamed Sultan Mohamed Ali and Dan Brox. Special thanks to all of them for being so supportive.

Last but not the least, my heartfelt gratitude goes to my wife, Parssa Hassan, for her loving encouragement and support; my mother, my father and all my family members for their mental support and inspiration.

DEDICATION

To my wife and parents

Chapter 1

Introduction

Conducting polymers possess various properties that are advantageous over conventional materials used in micro-electronics [1]. One notable feature is that their electrical conductivity can be electrochemically controlled (commonly reaching 10^4-10^5 S/m) [2, 3]. There are various applications of conducting polymers in micro-electronics, e.g., lithography, metallization, corrosion protecting coatings for metals and electrostatic discharge protective coatings for packages and housings of electronic equipment [3]. Conducting polymers have the potential to be used in interconnection technology and as novel organic materials in electronic devices [3]. Another important and promising application of conducting polymers is actuators. They are potentially suitable for medical applications such as surgical and diagnostic tools for minimally invasive surgery due to their features such as low actuation voltage, high strain, simple structure, and biocompatibility [4, 5]. Polypyrrole is one of the most commonly used conducting polymers as actuators [4]. High chemical and physical stability, low toxicity of monomer, and simple synthesis process make it competitive to other conducting polymers [6]. Polypyrrole actuators have been studied for a wide range of applications, including variable camber foils for underwater vehicles [7] and medical catheters [8, 9, 10]. The polymer was also reported for its application as immunosensors [11].

From a perspective of device fabrication and integration, it is essential to establish a micro-patterning method for this promising material with high precision, high throughput, and high repeatability. There have been various studies that investigated micro-machining of polypyrrole. Standard optical lithography technique was reported to pattern conductive polymer [12];

however there are concerns related to the chemical steps that may chemically damage the polymer or alter its properties. Patterned film of polypyrrole was obtained using pre-patterned metal electrodes through vapor-phase chemical polymerization with poor uniformity [13]. A self-assembled monolayer of polypyrrole was also reported [14]. However, the thickness of the layer achieved was only 1 μm, leading to smaller actuation forces and strains and thus limiting its application. There have also been reports on laser ablation of the polymer that was coated on medical catheters to produce isolated segments of the layer on the catheter [15]. This laser approach, however, typically exhibits low removal rates and thermal damages that lead to micro-cracks in the surface layer with debris deposited on the surface [15]. These issues can be mitigated using ultra-short pulse lasers [16]; however, there are still various issues, including precise depth control of the ablation, serial processing with limited throughput, and complex and expensive systems.

Micro-electro-discharge machining (μEDM) may be an alternative approach to micro-patterning of polypyrrole and other conducting polymers. This technique can be applied to any type of electrical conductors, including all kinds of metals and alloys as well as highly doped semiconductors. The material removal from a workpiece in the process is implemented by thermo-mechanical impacts that are created by pulses of miniaturized spark discharge, generated between a microscopic electrode and the workpiece that are usually submerged in dielectric liquid. Each discharge pulse, typically produced using voltages from 60 V to 100 V, produces significant heat at the discharge point, at which the surface layer of the material locally melts. Pressure waves created by instant evaporation of the dielectric fluid also caused by each pulse blow the molten portion off, leaving a crater-like shape on the surface. The machining process is achieved by repeating this single discharge removal at high frequencies (in MHz range). μEDM

is a non-contact micro-machining technique where a small discharge gap (typically one to a few μm, depending on the discharge energy) is maintained between the electrode and workpiece surface. This non-contact feature eliminates mechanical stresses applied to the workpiece, making the process possible in fragile and/or thin materials safely. Patterning in the μEDM process is performed by scanning a rotating cylindrical electrode, typically made of tungsten, using numerically controlled precision stages. Although the throughput in this scanning method is limited due to its serial processing nature, batch-mode μEDM using electrode arrays was demonstrated to enable parallel patterning for orders-of-magnitude higher throughput [17]. The versatility and large material base, high surface quality, no mechanical force, good repeatability, simple set-up and processing and minimum machinable size of 3-5 μm, with aspect ratio greater than 20, make the technique favorable over other micro-machining techniques. As polypyrrole has relatively high electrical conductivity (often 4×10^4 S/m or higher) [18], μEDM is potentially a suitable method to pattern the material with high precision, high throughput, and low cost. However, there has been little study on this possibility.

This thesis investigates and reports the feasibility of μEDM for patterning polypyrrole, its characteristics and actuation of catheters with μEDM patterned polypyrrole. The technical details of μEDM will be described in Section 1.1. Conducting polymers, their characteristics, application and patterning methods will described in section 1.2. Outline of the thesis will be discussed in section 1.3.

1.1 μEDM

μEDM has been endlessly evolving from a mere electrode and dies making process to a micro-scale application machining. In μEDM, the discharge energy is minimized in order to achieve micro-scale material removal. Since μEDM provides such advantages as the ability to manufacture complicated shapes with high accuracy, and can process any conductive materials regardless of hardness, it has become one of the most important methods for fabricating micro-features and parts with sub-micro-meter precision. μEDM has been applied in machining of hard materials for micro-molds and in the production of difficult-to-make features such as fuel injection nozzles, spinneret holes for synthetic fibers, electronic and optical devices, micro-mechatronic actuator parts etc. and also in fabrication of micro-tools for producing these devices [19, 20].

1.1.1 Historical Background of EDM and μEDM

In 1770, English chemist Joseph Priestly came to discover that electrical discharge or sparks had erosive effects and it is believed to be the basis of EDM [21]. In 1943, B.R. Lazarenko and N.I. Lazarenko at the Moscow University were able to use this sparks and developed resistance-capacitance type power supply to use with Lazarenko EDM System, which was able to machine difficult to machine materials in a controlled process by vaporizing material from workpiece surface [22]. The resistor-capacitor (RC) relaxation type pulse generator was extensively used at EDM machines in 1950s. At about the same time three American employees used electrical discharges to remove broken taps and drills from hydraulic valves. They were able to use electronic-circuit servo system which maintained space between electrode and workpiece automatically for sparks to occur [23]. In 1980, the introduction of computer numerical

controlled (CNC) in EDM has automated the EDM process. Therefore, after inserting the electrodes in Electrode changer, there is no requirement to monitor the process till the final product is ready [24]. Since then, EDM has been used in manufacturing industries and has become a topic of research. Through the years, the machines have improved drastically – progressing from RC power supplies and vacuum tubes to solid-state transistors with nanosecond pulsing, from crude hand-fed electrodes to modern CNC-controlled simultaneous six-axis machining. There has been widespread application of EDM in industry for last 70 years. However, the application of μEDM was demonstrated in 1968 for the first time [25]. A minute hole of several micro-meters (μm) was created in a 50-μm thick carbide plate. Since then, efforts on the research and development of micro-machining processes were undertaken. However, industrial application of micro-machining for production processes were not significant until recently as the demand for miniaturization shows an increasing trend. Since then, μEDM has become an important and cost-effective manufacturing process in machining parts, in the field of micro-electromechanical systems (MEMS), and in fabricating micro-features in difficult-to-cut materials [26].

1.1.2 Principles of μEDM

1.1.2.1 Mechanism of EDM and Application to μEDM

In EDM, a series of spatially discrete high-frequency electrical discharges (sparks) occur between the electrode and the workpiece [27]. When sparks are generated the electrical energy is converted to thermal energy and it erodes materials from electrode. Every discharge (or spark) melts or even vaporizes a small amount of material from both electrode and workpiece. During this process, electrons, emitted from cathode, move towards anode. After reaching anode, the electrons strike the anode surface and remove the metal ions from anode. Therefore, more

material is removed from anode surface. For this reason, the workpiece is generally used as anode and the electrode is used as cathode (negative polarity) [26]. Part of this material is removed by the dielectric fluid and the remaining material solidifies on the surface of electrode and workpiece. The net result is that each discharge leaves a small crater on both workpiece and electrode [28]. Fig. 1.1 explains the mechanism of EDM process. In the EDM process an energy column is formed as the electrode charged with a high-voltage potential come close to the workpiece. It eventually results in breakdown of the insulating properties of the dielectric fluid [29]. The voltage then drops as current is produced, and the spark vaporizes anything in contact with it, including the dielectric fluid. The area struck by the spark will be vaporized and melted, resulting in crater being formed. Thus metal is predominantly removed by the effect of intense heat locally generated and the collapse of the vaporized dielectric. Melting and vaporization actions are the causes of removal of material in the EDM process.

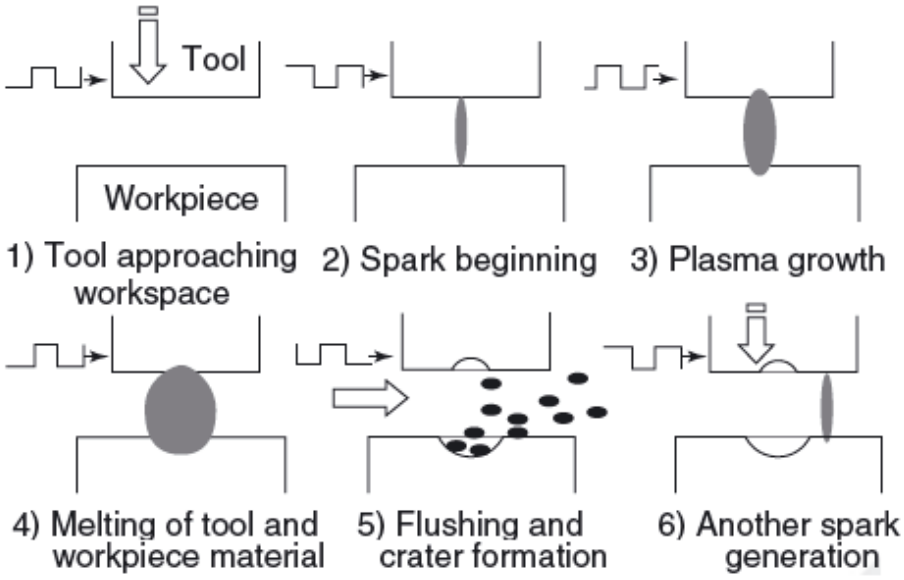

Fig. 1.1 EDM Process Mechanisms [20, with permission from Elsevier]

μEDM is based on the same physical principle as spark erosion. The basic mechanism of the μEDM process is essentially similar to that of the EDM process with the main difference being in the size of the electrode used, the power supply of discharge energy, the resolution of the X-, Y- and Z- axis movement, gap control and flushing techniques, and also in the processing technique [30]. In μEDM the discharge energy is reduced to the order of 10^{-6} to 10^{-7} Joules in order to minimize the unit material removal. Moreover, there are different processing techniques in μEDM that are not seen in conventional EDM. μEDM milling, wire electro-discharge grinding (WEDG) and repetitive pattern transfer are commonly employed in and more specific to the μEDM process [26].

1.1.2.2 Sparking and Gap Phenomena in μEDM

The sparking and gap phenomena during μEDM can be divided into three important phases, namely, preparation phase for ignition, phase of discharge, and interval phase between discharges [31]. In the preparation phase for ignition, an electric field or energy column is created with the application of gap voltage. This energy column gains highest strength at the closest distance between electrode and workpiece. The strength of the electrical field is high enough to break down the insulating properties of the dielectric fluid. In the discharge phase, when the resistivity of the fluid is lowest, a single spark is able to flow through the ionized flux tube and strike the workpiece. At this phase there is a drop in voltage as current is produced. The electrical energy is converted to thermal energy and the resulting spark vaporizes anything in contact, including the dielectric fluid, encasing the spark in a sheath of gasses composed of hydrogen, carbon, and various oxides. The area struck by the spark melts quickly and may even vaporize. At the interval phase between discharges, when the current is switched off, the heat source is eliminated and the sheath of vapor around the spark implodes. Its collapse creates a

void or vacuum and draws in fresh dielectric fluid to flush away debris and cool the area. Reionization also occurs, which provides favorable conditions for the next spark. Figure 1.2 illustrates the gap phenomena during the μEDM process.

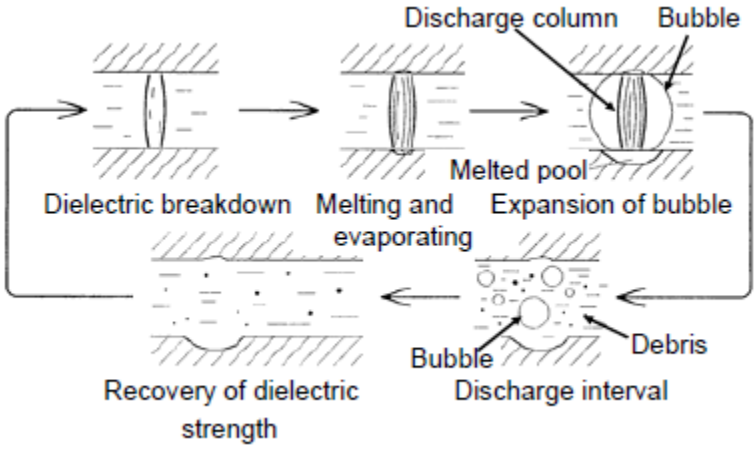

Fig. 1.2 Model of EDM Gap Phenomena [32, with permission from Elsevier]

1.1.3 Key System Components of μEDM

Initially, die-sinking EDM was used as a slicing machine for thin-walled structure. With the help of CNC, complex shapes can be cut without using special electrodes. The narrow spark gap and dimensional accuracy of the process make it possible to provide close fitting parts. Figure 1.3 shows the configuration of typical die-sinking EDM set-up.

An electrode replicates its shape on the workpiece. The workpiece can also be formed by three dimensional movement of electrode similar to milling process. The voltage and current, in the gap between Electrode and workpiece, is monitored by numerical control (NC). NC synchronously controls the different axes and the pulse generator from the feedback obtained

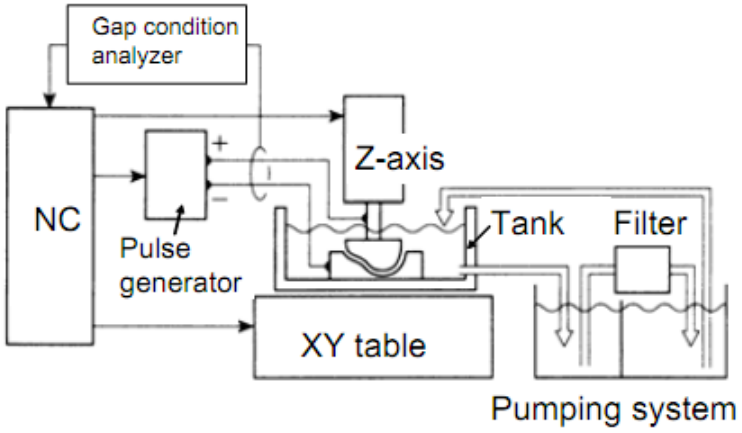

Fig. 1.3 Die-Sinking EDM Set-Up [32, with permission from Elsevier]

from gap condition analyzer. The dielectric liquid is circulated by a pumping system from a tank. A filter is placed inside the tank to remove debris particles and decomposition products from circulating dielectric fluid.

1.1.4 Types of Pulse Generators Used in μEDM

The controller circuit can have two types of pulse generators – RC relaxation type generator and transistor type generator. Based on research [33] and review [32], a description is given here on these different types of pulse generators. Two kinds of pulse generators: RC type pulse generator and transistor type pulse generator shown in Figures 1.4 (a) and (b) respectively. The fabrication of parts smaller than several μm requires minimization of the pulse energy supplied into the gap between the workpiece and electrode. This means that finishing by μEDM requires pulse duration of several 10's of nano-seconds. Since the RC pulse generator can deliver such small discharge energy simply by minimizing the capacitance in the circuit, it is widely applied in μEDM RC pulse generator results in extremely low material removal rate from its low discharge frequency due to the time needed to charge the capacitor.

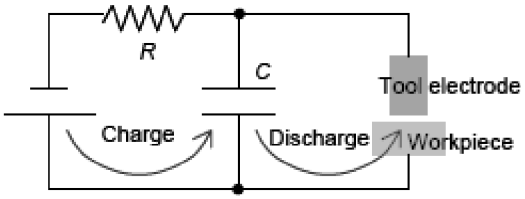

(a)

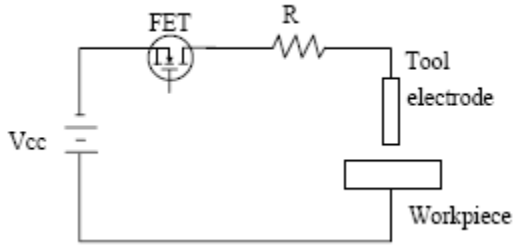

(b)

Fig. 1.4 Different Types of Pulse Generators (a) RC Type and (b) Transistor Type [33, with permission from Elsevier]

The transistor type pulse generator is on the other hand widely used in conventional EDM. Compared with the RC pulse generator, it provides a higher removal rate due to its high discharge frequency because there is no need to charge any capacitor. Moreover, the pulse duration and discharge current can arbitrarily be changed depending on the machining characteristics required.

RC type pulse generators were used in earlier EDM. The RC type was replaced by transistor type as the improved power transistors can handle large currents with high response. In RC type pulse generators, current continues flowing through the gap during a series of discharges. Therefore, there is always a presence of leakage current [34]. This leakage current does not allow the capacitor to be charged and results in interruption of pulse discharge [34]. The leak current generates joule heating at the discharging area and thus prevents the recovery of dielectric strength of the gap resulting in machining instability [34]. However, the RC type pulse generators are used in finishing and micro-machining because it is difficult to obtain sufficiently

short pulse duration with constant pulse energy using the transistor type pulse generator. If the transistor type is used, it takes at least several 10's of nano-seconds for the discharge current to diminish to zero after detecting the occurrence of discharge. The circuit for generating an output signal to switch off the power transistor and the power transistor itself has a certain amount of delay time. Hence, it is difficult to keep the constant discharge duration shorter than several 10's of nano-seconds using the transistor type pulse generator. To obtain smaller discharge energy per pulse in RC type pulse generators, the capacitance needs to be minimized as the discharge energy is equal to ½ CV^2, where C represents capacitance and V represents voltage of power source [35]. However, in an actual EDM setup, there is existence of stray capacitance (C_s) in the following areas [34]:

- In the circuit between the electric feeders
- Between the electrode holder and work table
- Between the electrode and workpiece

During EDM process, charge stored in C, together with C_s, is discharged in the working gap. Therefore, the discharge energy is equal to ½ $(C + C_s) V^2$, which is higher than the theoretical value obtained from ½ CV^2. Therefore, discharge energy can be reduced by using short electric feeders and by using electrical insulators for the electrode holder and work table. So, for final finishing with minimum discharge energy, EDM may be conducted with C_s only and C is not wired in the circuit. The RC type pulse generator has smaller C_s compared to transistor type, which is one of the main reasons for using RC type for micro-scale machining. Even after using short electric feeders, the stray capacitance cannot be completely eliminated. Moreover, there is also the existence of C_s between electrode and workpiece. With careful design of the equipment,

the value of C_s can be kept around 10-12 pF [36]. It is not possible to obtain discharge energy lower than ½ C_sV^2, which limits miniaturization in μEDM [30].

Another way of reducing discharge energy is to decrease the applied voltage. However, if the voltage is reduced, the gap width becomes narrow. Therefore, there is more possibility of frequent short circuit occurrence resulting in machining instability. It has been observed that in transistor type pulse generators, voltages below 60 V result in unstable machining [35, 37].

Machining of micro-rods of less than 1 μm diameter with EDM is difficult [38] as crater size of less than 2 μm diameter cannot be achieved due to the existence of stray capacitance (C_s) [39]. There have been reports of using scanning tunnelling microscopes for machining nano features in EDM with oil [40]. In this case, tunnelling current determines material removal rate instead of discharge current.

1.1.5 Types of Dielectric Media Used in μEDM

Hydrocarbon (kerosene) based EDM oil is generally used as dielectric medium in μEDM. The dielectric fluid enhances removal of debris without reattachment on the substrate and results in good surface finish [32]. It also avoids secondary discharges that can occur between electrode and workpiece due to deposition of debris on electrode [41]. This secondary discharge may results in higher electrode wear. Moreover, the flushing liquid also cools the machining area by removing debris that carries away a large portion of thermal energy. Therefore, it also reduces thermal damage on the workpiece.

In recent years, extensive research is going on to create machining technologies that are not harmful to the environment. Elimination of liquid or coolant as working media during these processes can be an important factor in this regard [42]. Therefore, using gas as dielectric

medium during EDM process can be considered as a relatively green technology. This method is considered as dry EDM. There has been report of achieving higher material removal rate by using oxygen as dielectric medium [43]. The material removal rate is low in non oxygen gas. Debris reattachment and odor of burning are the other two factors that limit the application of dry EDM [46]. Dry μEDM based on air and oxygen has also been applied to micro-patterning of carbon nanotube forest [44, 45].

The dielectric strength of liquid (>10MV/m) is higher than gas (<4 MV/m) [47]. Therefore, higher electric field is required to break down the dielectric strength of liquid dielectric media resulting in smaller gap distance between electrode and workpiece. Due to smaller gap distance between electrode and workpiece, the stray capacitance (C_s) between electrode and workpiece increases. Due to this higher capacitance, the minimum discharge energy increases [48]. Moreover thermal conductivity and heat capacity of liquid dielectric medium are higher than that of gaseous medium. This is an important factor that affects the solidification of debris and cooling of electrode and workpiece.

The feasibility of using combination of liquid and gases as dielectric medium was studied. Water mists in addition to air, nitrogen and argon gas were used as dielectric medium [49]. The liquid phase dispersed in a gas medium changes electrical field initiating easier discharge and larger gap distance [47]. This results in stable machining in lower energy. The debris reattachment can also be avoided as the liquid in the dielectric fluid flushes them away resulting good surface integrity [47].

1.1.6 μEDM and its Types

Current μEDM technology used for manufacturing micro-features can be categorized into different types [50]:

- Die-sinking μEDM, where an electrode with micro-features is employed to produce its mirror image in the workpiece.
- μ-wire EDM, where a wire of diameter down to 0.02mm is used to cut through a conductive workpiece.
- μEDM drilling, where micro-electrodes (of diameters down to 5–10μm) are used to 'drill' micro-holes in the workpiece.
- μEDM milling, where micro-electrodes (of diameters down to 5–10μm) are employed to produce 3D cavities by adopting a movement strategy similar to that in conventional milling.
- μWEDG (wire electro-discharge grinding) in which grinding is done using EDM mechanism.

Table 1.1 Overview of μEDM Varieties [20, with permission from Elsevier]

μEDM Variant	Geometric Complexity	Minimum Feature Size	Maximum Aspect Ratio	Surface Quality R_a (μm)
Drilling	2D	5 μm	~ 25	0.05 – 0.3
Die-Sinking	3D	~ 20 μm	~ 15	0.05 – 0.3
Milling	3D	~ 20 μm	~ 10	0.5 – 1
WEDM	2 ½ D	~ 30 μm	~ 100	0.1 – 0.2
WEDG	Axi-sym.	3 μm	30	0.8

1.1.7 μEDM Compared to Other Micro-Machining Processes

1.1.7.1 Advantages of μEDM over Other Micro-Machining Processes

Compared to traditional micro-machining technologies μEDM has several advantages [51]:

- EDM requires a low installation cost compared to lithographic techniques.
- EDM is very flexible, thus making it ideal for prototypes or small batches of products with a high added value.
- EDM requires little job overhead (such as designing masks, etc.).
- EDM can easily machine complex (even 3D) shapes.
- Shapes that prove difficult for etching are relatively easy for EDM.

1.1.7.2 Compatibility of μEDM with Other Micro-Machining Processes

Another important aspect of comparison between the micro-machining technologies is the compatibility of the machining technology with the material to be machined. μEDM has a strong advantage in the versatility of applicable materials that include all types of conductive materials such as metals, metallic alloys, graphite, or even some ceramic materials that have electrical conductance, of whatsoever hardness [30]. Table 1.2 gives an overview of the compatibility of the different micro-machining technologies [51].

Table 1.2 Compatibility of Micro-Machining Technologies with Different Materials [51, with permission from Elsevier]

Micro-Machining Technology	Feasible Materials
LIGA	Metals, Polymers, Ceramic Materials
Etching	Metals, Semiconductors
Excimer-LASER	Metals, Polymers, Ceramic Materials
Micro-Milling	Metals, Polymers
Diamond cutting	Non-Ferro Metals, Polymers
Micro-Stereolithography	Polymers
μEDM	Metals, Semiconductors, Ceramics

1.2 Conducting Polymers

The conductivity of conducting polymers can be adjusted in various methods. Some of these methods include chemical manipulation of the backbone structure, nature and degree of doping and addition of copolymers [3]. There have been reports of using Polypyrrole and Polyaniline as conducting polymer actuators [4].

1.2.1 Working Principle of Polypyrrole Actuators

Catheter is a hollow tube that is inserted into human body to perform common medical procedures such as providing a channel for fluid passage or an entry for medical devices [8]. In the conventional method, the catheter is inserted into the body passively by employing push/pull control mechanism from outside the body [52]. In this method, a wire is configured to be pushed or pulled along a longitudinal axis to bend the catheter tip. Long procedural time and risk of lumen or vessel wall damage have limited the application of this technique particularly when dealing with narrow passages. Conducting polymer actuators have attractive properties that make them are good candidates for converting passive catheters into active ones and controlling their manipulation inside the body [5]. In active element fabrication, the catheter is coated with polypyrrole forming trilayer structures, where two polypyrrole layers are electromechanically active material [53]. In their neutral state, these polymers are typically disordered semiconductor [54]. The effective bandgap can be reduced by addition (oxidation) or removal (reduction) of charges from the polymer chain which results in creation of states in the bandgap. Such a change in oxidation state in polypyrrole, induced electrochemically inside an ionic electrolyte is illustrated in Figure 1.5 (a) [8, 55]. In the process of changing oxidation state, dimensional

changes are observed. The mechanism of the dimensional change is illustrated in Figure 1.5 (b) [8, 55]. The trilayer structure with catheter and polypyrrole is submerged in an electrolyte solution containing mobile negative ions and large immobile positive ions. An alternating voltage is applied across the two polymer electrodes resulting in alternating oxidation and reduction of the polymer electrodes. As shown in Figure 1.5 (b), during oxidation of the right hand side polymer electrode mobile negative ions enter it from a surrounding electrolyte to balance charge. The negative ion insertion results in expansion of the right hand side polymer structure. Simultaneously, the left hand side polymer electrode is in the reduced state, where mobile negative ions exit the polymer to the surrounding electrolyte, which results in contraction of the left hand side polymer structure. Expansion on one side and contraction on the other side induces a stress gradient on the polymer/catheter interfaces and causes the whole structure to bend in one direction. This process reverses itself on the second half cycle of the alternating voltage, resulting in catheter bending in the other direction.

The electrolyte can be a liquid, a gel or a solid [5]. Solid polymer electrolyte is a complex of high molecular weight polymers and metal salts and a gel is a liquid solution of metal salts trapped in a cross-linked soluble polymer matrix.

In active element fabrication, chemical deposition is followed by an electrochemical deposition of polypyyrole on the catheter [8]. Four longitudinal stripes are cut in polypyrrole coating to create four electrodes [8]. Effective pattering of polypyrrole is a major issue for this kind of catheter actuation.

1.2.2 Other Applications of Polypyrrole

There have been reports of application of different shapes of polypyrrole for different purposes.

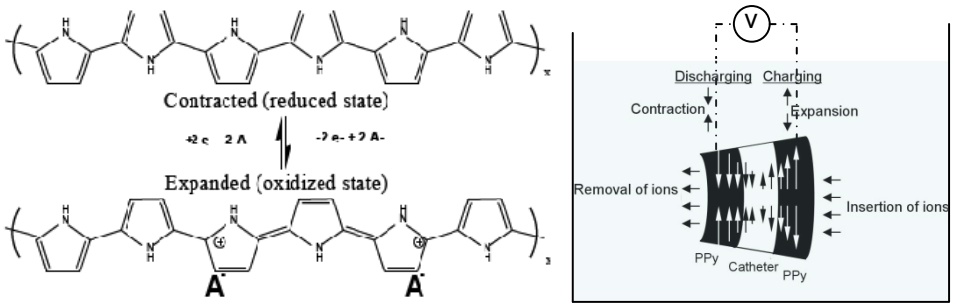

(a) (b)

Fig. 1.5 (a) Electrochemical Redox Cycle for Polypyrrole with Mobile Anions (A^-). (b) Stress Distribution upon Insertion and Removal of Ions from the Polypyrrole Layer.

[8, 55, with permission from SPIE]

Polypyrrole nanowire arrays provides high surface to volume ratio [56]. Based on these phenomena, a highly responsive ammonia gas sensor was established [56]. Three dimensional micro-porous polypyrrole structures provide extremely high surface area [57]. They can promote interaction with cells and improve the interface of neural electrode and tissue [57]. As a scaffold for cell growth, there have been reports of using honeycomb structured polypyrrole films [58]. In comparison to unmodified polypyrrole, striated polypyrrole films demonstrated better nerve growth [59]. Electrolyte filled pores in polypyrrole has the ability to reduce ion diffusion paths resulting in improvements of the electrochemical strain rate of the actuator [60].

1.2.3 Summary of Patterning Techniques Reported for Polypyrrole and Other Conducting Polymers

As noted earlier, several techniques have been reported for patterning polypyrrole. A standard lithography technique has been used to pattern conductive polymer. Photoresist deposited on the

surface is patterned by UV light resulting in soluble and insoluble parts [12]. The soluble parts are removed by the appropriate solvent. However, there is possibility of solvents dissolving and swelling the polymer, chemicals altering the structure and ultra-violet (UV) light causing degradation [12]. Thin patterned films of polypyrrole can be obtained on patterned metal electrodes by chemical polymerization from vapor phase [13]. Sputtered copper reacts with chlorine vapor and form chlorinated salt. Chemical vapor deposition of polypyrrole occurs after this process. However, the polypyrrole layer formed in this process is not uniform [13]. A micro-patterned self assembled monolayer has been used to define areas favorable or unfavorable for polymer deposition [14]. A pattern of alkanethiols was defined by micro-contact printing on gold. The substrate was immersed in a solution of short-chain alkanethiols. Polypyrrole were preferentially deposited on the regions covered by short chains. A 1-μm-thick film with 6 μm line widths was defined in this method [14]. Micro-contact printing [61, 62] and vacuum assisted micro-molding [63] have also been employed for micro-patterning of polypyrrole. However, all these methods involve multi step procedures with finely patterned master template and planar rigid substrates [64]. Contactless patterning of polypyrrole using KrF excimer laser has also been demonstrated to remove polypyrrole from cylindrical catheter creating electrically isolated strips [15]. However, large heat and shock affected zones are created due to material interactions with pulse duration higher than 10 ns [64] which is the case for the excimer laser. This resulted in degradation of machining precision. Moreover, beam geometry was not flexible so that it can be projected upon a large area for processing a non planar surface [64]. This resulted in higher processing time. Ultra-fast micro-machining of polypyrrole with a femtosecond pulse laser was also demonstrated recently with strong non linear interaction, small heat affected zones and high resolution surface micro-patterning [64]. However, these ultra-short

pulses remove materials through serial processing and require higher purchase cost, maintenance cost and complex optical component for beam alignment [65, 66, 67].

1.2.4 Polypyrrole Patterning by μEDM – Feasibility Consideration

μEDM has been employed in shaping metals. Most of these metals have conductivity in the range of 10^5 – 10^7 S/m [68]. However, there has been report of shaping ceramics with μEDM. The electrical conductivity of ceramics ranging between 0.33 S/m- 1 S/m is the main obstacle to shape them using μEDM [69]. It has been demonstrated that SiC (conductivity 20 S/m) and B_4C (conductivity 100 S/m) can be shaped by μEDM [70]. However, there is a small transition zone between stable machining and unstable machining for a low electrically conductive material. Stability regions are identified as discharge current, discharge duration and pulse interval [70].

In μEDM, electrical energy is converted to thermal energy and material removal takes place through thermal erosion. Therefore, there may be concern of thermal damage on the surface, which is also a potential case for polymer patterning. However, in μEDM, not all of the thermal energy is transferred into the cathode or anode. For short discharge duration, a larger fraction of the total energy is consumed to generate plasma and increase enthalpy of the plasma [71]. Only 10-15% of the total energy is transferred to the cathode and anode [71]. Moreover, a major portion of the energy is carried away by debris. When the removal mechanism is dominated by vaporization rather than melting, energy carried away by debris will be maximum, considering consumption of more energy for vaporization [71]. Under these conditions, polypyrrole might be processed by μEDM with minimal thermal damage as thermal energy deposited to polypyrrole can lead to instant vaporization of the material.

As polypyrrole and other conducting polymers have higher conductivity than ceramics but lower conductivity than metals, it is worth studying the feasibility of μEDM for these materials. However, to the best of author's knowledge, there has been no study on μEDM of polypyrrole and other conducting polymers. In general, the material removal rate in μEDM is slow. However it can be increased through batch-mode processing [17]. The availability of μEDM for polypyrrole patterning will address the difficulties associated with other micro-machining techniques outlined above and open many paths to engineering applications of the material including medical devices such as active catheters.

1.3 Outline of Thesis

The entire thesis is organized in the following order: Chapter 2 describes the experimental preparation and setups. It includes details of the μEDM machine, electrode material and dielectric medium, electrode shaping and experimental parameters used in this study. It describes the polypyrrole growth as thin film and its deposition on catheters. It also illustrates the details of all the experiments conducted. In the final part, it provides a brief description of the measurement apparatus. Chapter 3 characterizes different structures machined on polypyrrole with μEDM using various methods (die-sinking, milling) and dielectric media (air, EDM oil). It also demonstrates variation of discharge current with different modes of contact of polypyrrole films on conductive substrates and the effect of single discharge phenomena on polypyrrole films. Energy Dispersive X-ray (EDX) is also performed for elemental analysis of polypyrrole before and after EDM process. The final part demonstrates the application of μEDM to pattern polypyrrole deposited on a catheter and actuation of the catheter. Chapter 4 concludes this study with recommendations.

Chapter 2

Experimental Preparation and Set-Ups

A series of experiments were conducted to study the feasibility of micro-patterning of polypyrrole using μEDM. This chapter describes the experimental set-up and procedures for patterning of planar polypyrrole films and polypyrrole deposited on cylindrical catheters; deposition of polypyrrole films and polypyrrole electrode on catheter; and medium and mechanism of catheter actuation.

2.1 μEDM

2.1.1 μEDM Machine and WEDG Module

To conduct μEDM on polypyrrole, a commercial μEDM machine (EM203, SmalTec International Inc., IL, USA) shown in Fig. 2.1 has been used. The positioning range of the machine is 200 mm (X) × 200 mm (Y) × 95 mm (Z). The X-Y stage is used to position the sample laterally, and the Z stage is to feed the electrode into the sample vertically. During a process, the system continuously monitors a short circuit between the electrode and the sample; upon the detection of a short circuit, the system automatically retracts the electrode upward and once the short circuit is cleared, it resumes feeding of the electrode. For positioning detection of X and Y axis, there is a glass scale readout of 0.1 μm. Minimum travel resolution for all the axes is 0.1 μm. Maximum rotation speed of electrodes is 6000 rpm. The accuracy is around 1 μm for 10 mm targeted values and 5 μm for 100 mm targeted values.

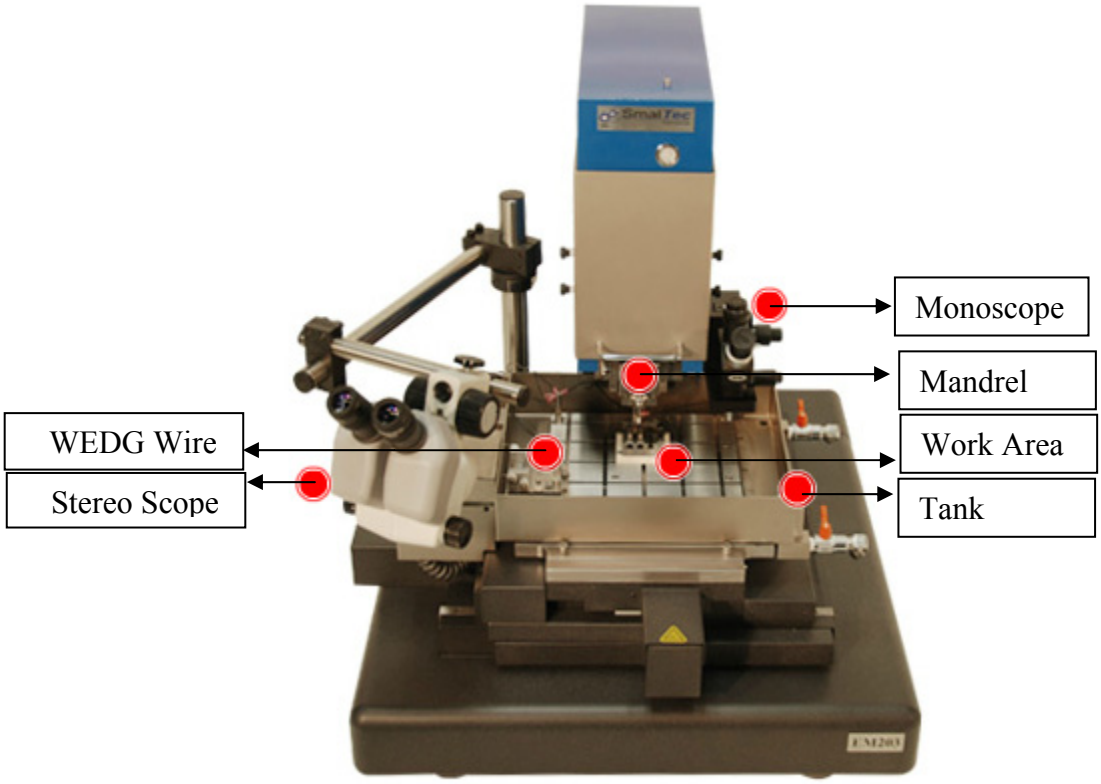

Fig. 2.1 Overview of SmalTec EM 203 µEDM Micro-Grinding Machine

(with permission from SmalTec International)

Detailed description of the components is given below:

Mandrel: It acts as a holder and spindle. It allows quick removal and precise placement of spindle.

Work area: It is made of stainless steel with less than 10 µm flatness.

Monoscope: It allows optical alignment of workpiece.

Tank: It allows flooded or flushed flow of dielectric or deionized water.

WEDG Wire: A precision brass wire of diameter tolerance of less than 1 µm is used for shaping electrodes.

Stereo Scope: It is used to view the process and rough alignment of workpiece and electrode.

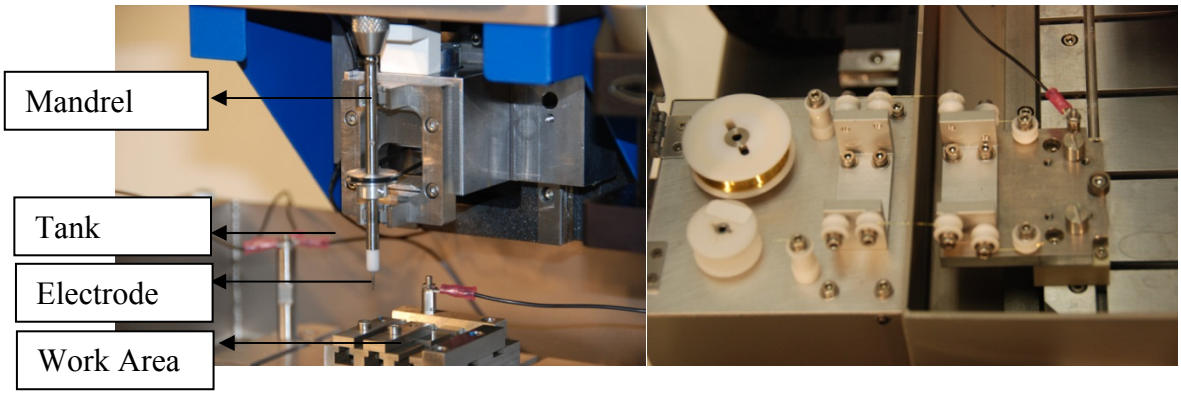

(a) (b)

Fig. 2.2 Detailed Image of SmalTec EM 203 µEDM Micro-Grinding Machine (a) Mandrel, Work Area and Tank (b) WEDG Wire (with permission from SmalTec International)

2.1.2 Electrode Material

Tungsten wire of diameter 300 µm has been used as electrode in this study. Negative polarity of the electrode is selected to conduct experiments following to the typical configuration discussed in previous section. Tungsten is the most commonly used electrode material in µEDM because of its high mechanical stiffness, high melting point (3422 °C) and good conductivity. Properties of tungsten are given in Table 2.1.

2.1.3 Dielectric Liquid

Commercial EDM oil (EDM185, Commonwealth Oil, Canada) is used as the dielectric liquid medium in this study. This dielectric fluid, based on kerosene as in most of other EDM oils, is

Table 2.1 Properties of Tungsten [72]

Property	Unit	Value
Density of Solid	g/cm^3	19.25
Modulus of Elasticity	GPa	390-410
Hardness	HV30	300-650
Electrical Resistivity	μΩ.cm	5.28
Heat Capacity	KJ/(mol.K)	24.10-24.42
Thermal Conductivity	W/(cm.K)	1.75
Coefficient of Thermal Expansion	$10^{-6}/K$	4.32-4.68
Melting Point	°C	3422±15

odorless and ideal for very fine work with tight tolerances. Very low viscosity of this fluid enables rapid flushing at point of machining and is suitable for micro-scale processing. This fluid is compatible with all standard filtration method and free from halogens, solvents, PCB's and ozone depleting compounds. This dielectric is cleaner and clearer and has longer fluid life. Properties of EDM 185 are shown in Table 2.2.

2.1.4 Experimental Procedure

2.1.4.1 Electrode Shaping Using WEDG

Electrodes used in this study ranged from 300 μm to 20 μm. WEDG available with the EDM setup was used to shape the 300 μm diameter tungsten wire into different diameters as well as to flatten the bottom surface of electrode. WEDG with one wire guide is attached to μEDM machine. The main machining steps are bottom flattening of electrode and shaping electrodes to

Table 2.2 Properties of EDM 185 Dielectric Fluid

(with permission from Commonwealth Oil Corporation)

Appearance	Clear
Density	6.639 lbs./US gallon
Specific gravity	0.798
Viscosity at 25^{o}C	2.20 cSt
Flash point COC	82 ^{o}C
Odor	Nil
Saybolt color	30+

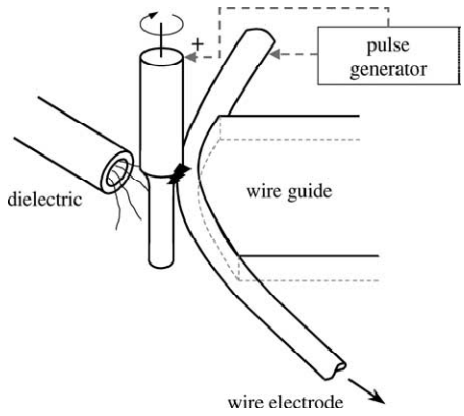

Fig. 2.3 Schematic of WEDG [73, with permission from Elsevier]

a smaller diameter. Fig. 2.3 depicts the schematic of WEDG process with one wire guide [73]. It can shape electrodes with flexible geometry. For shaping, the electrode material is taken near the WEDG setup with movement of X and Y axis. Then Z axis is moved down using the stereoscope. The polarity of electrode is positive and WEDG wire (brass) is negative as removal takes place on the electrode material. The WEDG was performed with parameters as described in

Table 2.3. The electrode with 300 µm diameter was shaped to 100 µm. After using 100 µm diameter electrode, this electrode was shaped to 50 µm and was used for EDM. Finally this 50 µm diameter electrode was shaped to 20 µm diameter and used to pattern structures. Fig. 2.4 shows the optical image of the shaped electrodes.

Table 2.3 Parameters for WEDG

Dielectric	EDM oil
Resistance (KΩ)	1
Capacitance	213.3 pF (bottom flattening), 3.27 nF (shaping)
Voltage (V)	80
EDM Feeding Speed (Z, mm/min)	0.05 (bottom flattening), 0.1 (shaping)
Scanning Speed (X, mm/min)	10 (bottom flattening)
Spindle Rotation Speed (rpm)	4000

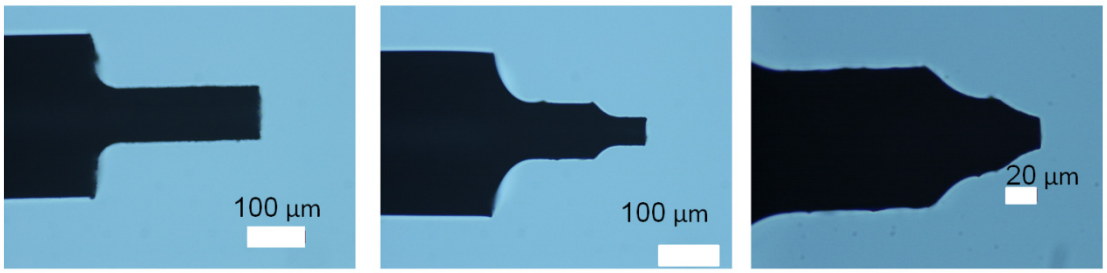

(a) (b) (c)

Fig. 2.4 Optical Images of Shaped Electrodes of Diameter (a) 100 µm (b) 50 µm and (c) 20 µm

2.1.4.2 Machining Parameters

Machining was conducted using various combinations of voltage and capacitance in RC type pulse generator using air and EDM oil as dielectric medium. Table 2.4 lists the parameters used in the experiments.

Table 2.4 Parameters Used in Machining

Dielectric	Air, EDM oil
Resistance (KΩ)	1
Capacitance	10 pF(Air, EDM oil)) Stray Capacitance, 100 pF (EDM oil) 213.3 pF (Catheter with EDM oil) 330 nF (Single Discharge)
Voltage (V)	20, 30, 40 (Air) 60,80,100 (EDM oil) 120 (Catheter with EDM oil, Single Discharge)
EDM Feeding Speed (Z, mm/min)	0.03(polypyrrole films), 0.05 (Catheter)
Scanning Speed (X&Y, mm/min)	4
Spindle Rotation Speed (rpm)	4000
Electrode (-ve polarity)	Tungsten (Diameter in μm) 20, 50,100 and 300

2.2 Polypyrrole Preparation

2.2.1 Film Growth for Micro-Patterning Experiments

Polypyrrole in the form of film was used for patterning experiments with μEDM. Polypyrrole was grown on a substrate by polymerizing pyrrole monomer through electrochemical oxidation. Fig. 2.5 shows the set-up for electrochemical deposition. The substrate where the polypyrrole deposition will occur is known as working electrode. Glassy carbon crucible is used as working electrode with positive polarity. Polished copper is used as counter electrode with negative polarity. The working electrode is firstly polished with Alpha Micro-polish 2. To grow

polypyrrole films the procedure described by Yamaura was followed [74]. According to this procedure, a solution of 0.06 M pyrrole monomer [C_4H_4NH], 0.05 M tetrabutylammonium hexafluorophosphate [$(CH_3CH_2CH_2CH_2)_4N^+$ $(PF_6)^-$] and 1% vol. distilled water in propylene carbonate [$C_4H_6O_3$] are mixed and blend together. Magnetic spinner and Nitrogen bubbles are employed to mix it properly. Then the solution is chilled to -40 ºC. A polished copper counter electrode and a current density of 0.125 mA/cm^2 is used for electrochemical deposition. 8 hours of deposition time generally yields 10 µm - 15 µm thick polypyrrole. After deposition of polypyrrole on glassy carbon crucible, it is dried overnight. Once dried, the deposited polypyrrole is peeled off the crucible and used for patterning.

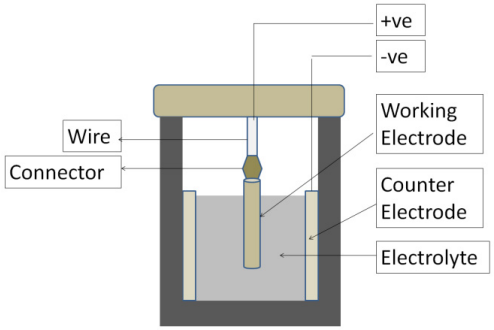

Fig. 2.5 Set-Up of Electrochemical Deposition

2.2.2 Film Growth on Catheter Samples

Toward application of the technique for fabrication of active catheters, samples of polypyrrole film coated on actual catheters were prepared. The catheter used in this study was a Prowler® Select® LP ES Micro-Catheter with outer and inner diameters of 0.75 mm and 0.42 mm respectively. Polypyrrole was deposited on the catheter in two steps: (i) electroless deposition for seed layer formation and (ii) electrochemical deposition for the polypyrrole film growth. For electroless deposition, two types of solution were prepared. In oxidation solution, 1.2 gm of

ferric chloride [$FeCl_3$] is added to 0.1 M of hydrochloric acid [HCl]. In pyrrole solution, 0.001 M pyrrole [C_4H_4NH] was added in 10 mL of deionized water. The catheter is dipped in oxidation and pyrrole solution in sequences for several times in order to deposit a thin layer of polypyrrole on catheter that acts as the seed layer. Polypyrrole is then electrochemically grown onto this seed layer using the method described in section 2.2.1

2.3 Experimental Set-Up and Procedure

µEDM of polypyrrole was investigated in several steps. Fig. 2.6 shows the schematic diagram of the µEDM of polypyrrole films with current probe to measure discharge current.

The Machining details of several phases are described below:

µEDM in air

Phase 1: The feasibility of µEDM of polypyrrole films were investigated with drilling of micro-through-holes in air as dielectric medium. Voltages of 20 V, 30 V and 40 V were used with 10 pF capacitance. The diameter of tungsten electrode was 300 µm.

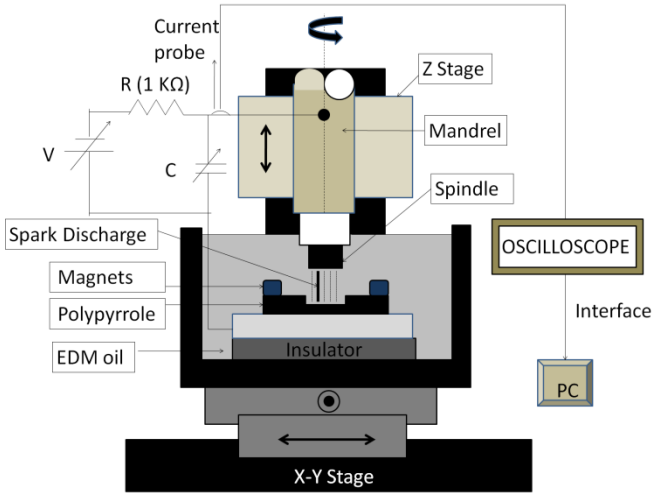

Fig. 2.6 Schematic Diagram of µEDM of Polypyrrole Films

Phase 2: Die sinking EDM for making holes with bottom layers were conducted with same parameter used in drilling of through-holes, using 150 μm diameter electrode. The depth was reduced to 5 μm so that the structure of polypyrrole after EDM can be observed.

Phase 3: Milling EDM with bottom layers, using 100 μm diameter electrodes, were performed. The electrode scanned along a lateral axis for a distance of 200 μm while feeding to a depth of 10 μm with the same machining parameters and ambient (air).

μEDM in oil

Phase 4: EDM oil was used as dielectric medium. Stray capacitance and 10 pF were used with 60 V, 80 V, 100 V and 120 V. 100 μm diameter electrodes were used for milling EDM of 200 μm.

Phase 5: Electrodes were shaped to 100 μm, 50 μm and 20 μm to create square structures with length of the sides being 300 μm, 150 μm and 60 μm respectively. 60 V and C_s were used with EDM oil.

Phase 6: Polypyrrole was connected to conductive surface in three different modes and discharge current was measured for 60 V and stray capacitance. Electrodes of 100 μm diameters were used for milling EDM of 200 μm lengths. In Mode-1 Polypyrrole film was placed on conductive surface. In Mode-2, Polypyrrole was fixed on dielectric and conductive connector was connected to polypyrrole films with μEDM performed at 7.3 mm far from connector. In Mode-3, Polypyrrole was fixed on dielectric and conductive connector was connected to polypyrrole films with μEDM performed at 3.5 mm far from connector. The contact resistance was also measured for different modes. These parameters were used in LT Spice simulation to find the simulated values of currents for three different modes of contact. The stray capacitance was assumed to be 10 pF for simulation purpose.

Phase 7: EDM circuit was developed in a bread board with 1 KΩ resistance, 3.30 nF capacitance and two switches. An external DC power supply of 120 V was used. This circuit was connected with electrode and workpiece holder of EDM machine. This circuit was used to observe the effect of single discharge on polypyrrole and stainless steel.

Phase 8: Polypyrrole deposited on catheter was removed using μEDM. Electrodes of 300 μm diameter were used with 120 V and 213.3 pF. EDM oil was used as dielectric medium and depth of machining was 60 μm. After removing polypyrrole from one side of catheter, it was rotated 180 degree and polypyrrole was removed from other side resulting in catheter with two electrodes.

Phase 9: Catheter, patterned with two polypyrrole electrode, was actuated. An aqueous solution of $NaPF_6$ was used to actuate 10 mm long catheter .The actuation potential was a step voltage of ±8 V across the two polymer electrodes. Ag/AgCl was used as reference electrode.

2.4 Measurement Apparatus

2.4.1 VP SEM with EDX (Hitachi S3000N)

The scanning electron microscope (SEM) used for imaging can be used in high vacuum and variable pressure modes with a range from 5 Pa to 270 Pa. It utilizes conventional Tungsten filament electron gun and can be operated at acceleration voltage up to 25 KV. In high vacuum mode, the system is capable of imaging at a resolution of 3 nm (15 nm at 3 KV). In variable pressure mode, the system is capable of imaging at a resolution of 4nm using the backscatter detector. Variable pressure capability allows the imaging of insulating samples that would otherwise require coating. It also includes an energy dispersive X-ray (EDS/EDX) detector which allows semi quantitative and quantitative elemental compositional analysis.

2.4.2 Surface Profilometer (Dektak 150, Veeco, USA)

Dektak 150 surface profilometer was used to measure the surface profile of polypyrrole after μEDM. Average surface roughness (R_a) was also obtained from Dektak software. The radius of the stylus is 12.5 μm and stylus force is 1-3 mg.

2.4.3 Nikon Measuring Microscope (MM 400/L)

Nikon MM 400/L is used to measure electrode diameter after shaping and also to verify the machined structures after μEDM before taking SEM images. This microscope has built in Z linear scale and high intensity white LED illuminator. This microscope is coordinated with data processor DP-E1. This data processor has a 0.1 μm-reading counter display. Illumination, X/Y stage and Z data is also connected to the MM Controller as an interface to an external computer running E-Max software for data processing and system control. This microscope has DS-2Mv Nikon digital camera featuring a 2-megapixel CCD.

2.4.4 Current Probe (CT-1, Tektronix, USA)

The CT1 probe consists of an inductive current transformer and an interconnecting cable. The current transformer has a small hole through which a current carrying conductor is passed during circuit assembly. The P6041 Probe Cable provides the connection between the CT1 current transformer and an oscilloscope input. A 50 Ω termination is required to terminate the cable when connected to a high-impedance (1 MΩ) oscilloscope input. The CT1 provides an output of 5 mV for each milliamp of input current when terminated in 50 Ω.

2.4.5 Infiniium Oscilloscope (54845A, Agilent Technologies)

The oscilloscope is used to capture waveforms with 1.5 GHz bandwidth and 8 GSa/s sample rate.

Chapter 3

Results and Discussions

In EDM, values of various parameter affect the machining characteristics. One of the main objectives of this study is to find optimum parameters and effective flushing medium for patterning polypyrrole with higher machining precision and surface quality. Since lower energy is required for minimal surface damage, smaller values of capacitance and voltage were employed. Micro-holes and micro-slots were patterned on polypyrrole. Based on the optimum parameter, rectangular structures of different dimension were patterned. The performance parameters were measured in terms of average surface roughness, surface integrity, spark gap, depth control, machining stability, peak current, pulse duration and frequency. These experiments were done using a RC type pulse generator. Two types of μEDM modes, drilling and milling, were conducted. Two types of dielectric media, air and EDM oil, were investigated in this study. Experiments were also performed to observe the effect of a single spark on polypyrrole during the process. Polypyrrole was also connected in different modes of contact and currents were measured to observe the effect of contact methods of polypyrrole. SPICE Simulation was also conducted to simulate the currents in different modes of contact. Finally, μEDM was employed on patterning polypyrrole on catheter and the patterned polypyrrole was used as active element for catheter actuation.

3.1 Polypyrrole μEDM in Air

3.1.1 Drilling of Micro-Holes

To assess the feasibility of polypyrrole removal with the μEDM principle, the machining tests were first performed in air as the dielectric medium of the process. A 300-μm-diameter electrode was used to create micro-holes on polypyrrole using different combinations of voltages and 10 pF capacitance. It was evident that the set-up produced discharge pulses that caused removal of the material while the electrode was fed into the material. To observe the effects of discharge voltage on the removal of the material, varying voltages of 20 V, 30 V and 40 V (with a fixed capacitor of 10 pF) were applied across the electrode and the workpiece. Fig. 3.1 shows sample through-holes produced in this test. The results clearly show that μEDM is effective in creating micro-structures in polypyrrole while transferring the pattern of the electrode to the material. When lower energy is used, there is less thermal damage on the periphery of micro-holes. As can be seen from Fig. 3.1, 40 V resulted in more thermal damage on the surrounding area of the micro-hole. To observe the effect of lower energy on the edges of the hole, SEM images of the edges were captured. It can be seen from Fig. 3.1, lower voltage resulted in smoother edges.

3.1.2 Die-Sinking μEDM with Bottom Layers

In order to find the effect of EDM with air on surface of polypyrrole, die-sinking EDM for creating holes with bottom layers was conducted using 150 μm diameter electrode and the same parameters used for micro-holes. The depth was reduced to 5 μm so that bottom layers were left in the holes and the surfaces of polypyrrole after EDM can be easily observed. Fig. 3.2 shows the SEM images of two circular structures.

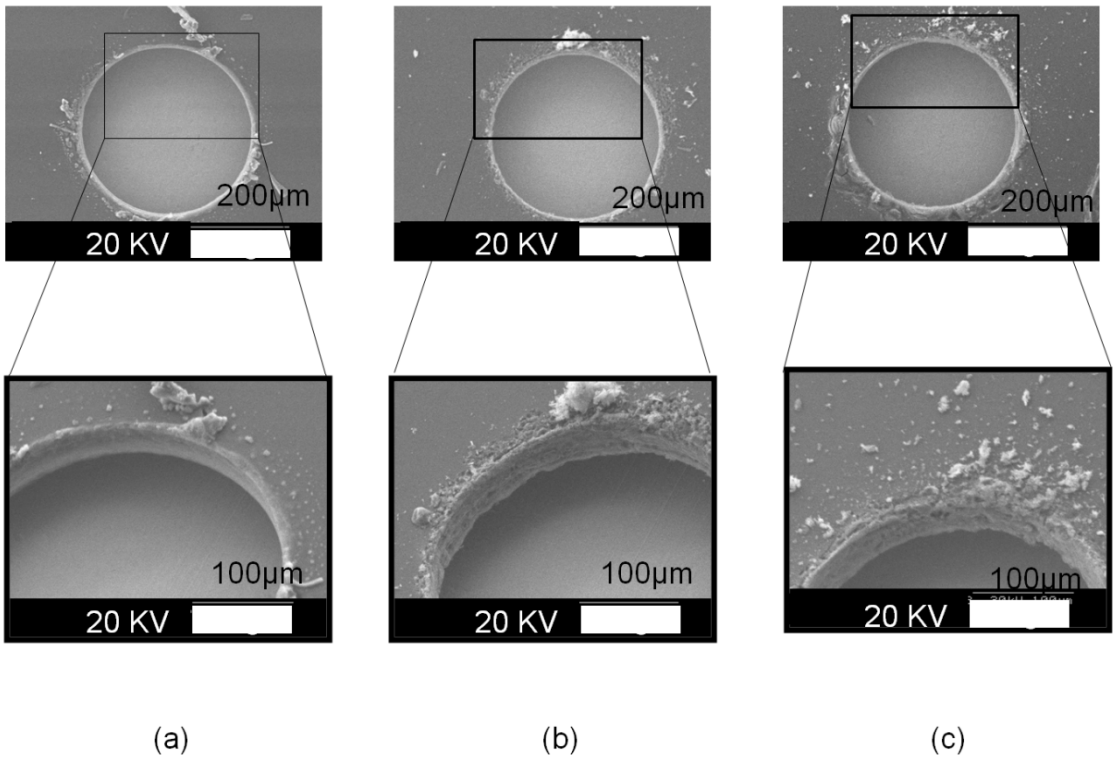

Fig. 3.1 SEM Images of 300 µm Holes on Polypyrrole with 10 pF and (a) 20 V (b) 30 V (c) 40 V

It can be seen from Fig. 3.2, there is evidence of micro-cracks and materials attached to the surface of polypyrrole. EDX was performed in selected areas as marked in Fig. 3.2. Table 3.1 shows the EDX analysis of those areas. It was observed from Table 3.1 that there is evidence of tungsten; this suggests that the electrode material was melted and attached to the surface during the process. This is likely caused by the condition that there was no flushing dielectric to reduce the heat generated in that area. Given this result, the next test focused on whether milling can improve the condition as the electrode is on movement in X or Y axis and not confined to a certain area.

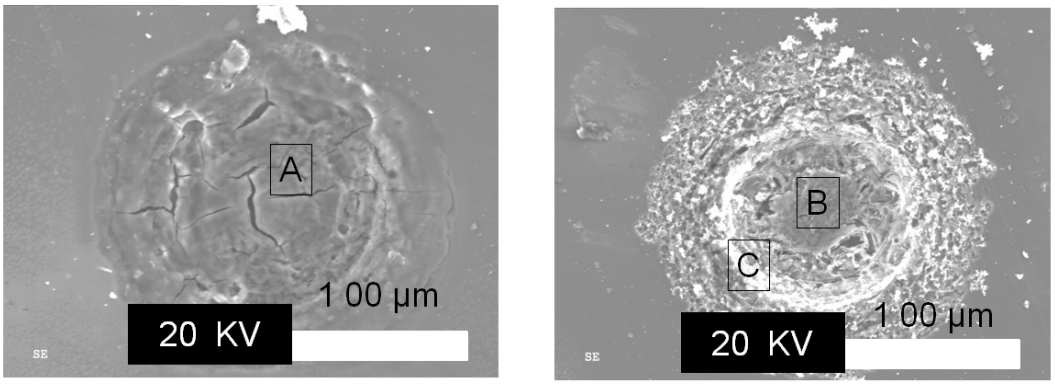

(a) (b)

Fig. 3.2 SEM Images of 150 µm Circular Structures on Polypyrrole with 10 pF and (a) 20 V (b) 30 V

Table 3.1: EDX Analysis on Circular Structure with EDM in Air

Elements	A	B	C
Carbon	35.86 wt%	31.23 wt%	35.08 wt%
Nitrogen	14.67 wt%	19.64 wt%	13.59 wt%
Oxygen	36.78 wt%	36.09 wt%	36.32 wt%
Fluorine	3.72 wt%	1.51 wt%	0.81 wt%
Phosphorus	8.71 wt%	10.68 wt%	12.34 wt%
Aluminum	0.27 wt%	0.33 wt%	0.20 wt%
Tungsten	**0 wt%**	**0 wt%**	**1.67 wt%**

3.1.3 Milling μEDM with Bottom Layers

For this test, slot structures with bottom layers were patterned using the 100 μm diameter electrode that was scanned along a lateral axis for a distance of 200 μm, while feeding electrode to a depth of 10 μm, with the same machining parameters and ambient (air). The results shown in Fig. 3.3 indicate micro-cracks on the patterned polypyrrole, even at lower voltages. This may be attributed to the processing in air, in which the effect of debris flushing may not be sufficient even in this milling/scanning process. Produced debris might have caused electrical paths for short circuiting between the electrode and the workpiece, potentially causing thermal damages including the micro-cracks on the processed surfaces.

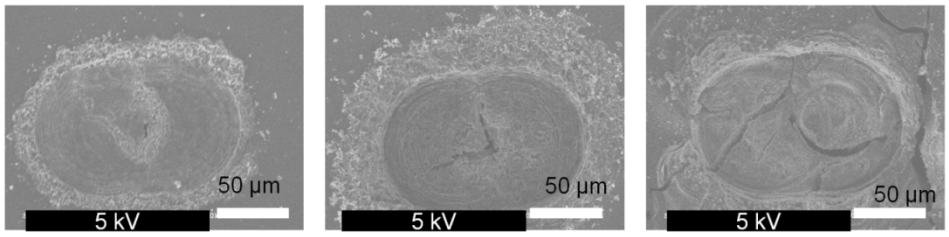

Fig. 3.3 Dry EDM of 300 μm Slots Using 100 μm Electrode with10 pF and

(a) 20 V (b) 30 V (c) 40 V

3.2 Polypyrrole μEDM in Dielectric Oil

3.2.1 Milling μEDM with Bottom Layers

Following the previous test with air, the effect of using liquid ambient, specifically EDM oil, on the process was studied, based on a presumption that it will provide higher flushing effect, similar to typical μEDM processes, compared to the case in air.

The diameters of electrodes and pattering length and depth similar to those used for the tests in air were employed in this experiment in oil. However, it was observed that the EDM parameters that led to stable discharge were slightly different from those used for the process in air. In particular, higher voltages were required to generate spark pulses in a stable manner. This result may be attributed to the fact that dielectric strength of EDM oil is higher than air. This, in turn, means that the required energy for dielectric breakdown is higher in the case of oil compared with the case of air. In order to characterize the effect of voltage and capacitance on the machining characteristics, firstly voltage was kept constant (60 V) and capacitance was varied (C_s only, C=10 pF, and C= 100 pF). Then the capacitance was kept minimum (C_s only) and the voltage was varied (60 V, 80 V, and 100 V). The electrode was fed into the material with a 0.5 μm step along the Z direction. In this process, a targeted depth of 10 μm was machined.

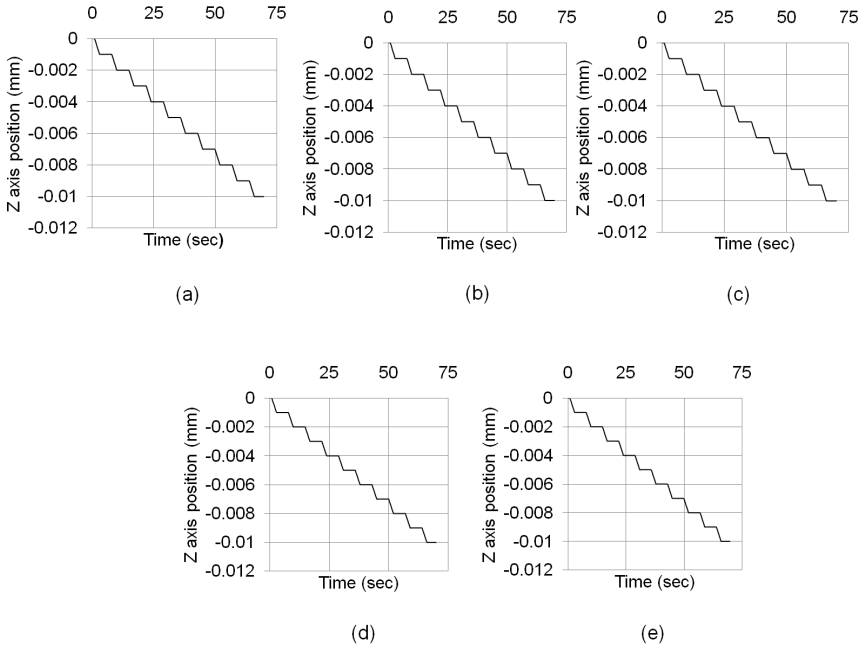

Fig. 3.4 Position of Z Axis with Machining Time for Linear Structure with (a) 60 V-C_s (b) 60 V-10 pF (c) 60 V-100 pF (d) 80 V-C_s (e) 100 V-C_s

To visualize the machining progress, the position of Z-axis with time was recorded during the machining process. As can be seen from the results for different parameters shown in Fig. 3.4, the Z axis moved downward without any retracting motion, indicating stable removal processes without short circuiting.

Fig. 3.5 depicts the SEM images of polypyrrole structures machined using these conditions. It can be seen, that 60 V and C_s resulted in better surface structure with no burrs around the machined area. In contrast, the structure with 10 pF and 100 pF (Figs. 3.5 (b) and (c), respectively) resulted in damage around the surrounding area. This damage appears like portions of the surface layer that were peeled but still connected to the edges of the patterns. This large "burrs" on the edges can be seen more for the pattern made with 100 pF. The mechanism of this burr formation is not clear. It may be attributed to the condition that although the discharge energy was increased with capacitance, the machining gaps remained small in all these cases as the lowest voltage level (60 V) was commonly used. This situation may have led to more accumulation of heat in the processing region (more for the 100 pF case) and potential thermal alteration of the material properties, specifically electrical conductivity. It was reported that the electrical conductivity of polypyrrole rapidly dropped when heated beyond ~150 °C [75]. This hypothetical condition can affect proper generation of discharge pulses and could cause partial mechanical scratching rather than EDM, leading to large burr formation. (Note if the material conductivity is not sufficient, the system cannot detect short circuits, and thus may show smooth feeding of the electrode as shown in Figs. 3.4(b) and (c)).

The results shown in Figs. 3.5(a), (d), and (f) indicate that the increase of voltage (with common stray capacitance) did not cause large burrs observed above in the case with increased capacitance, providing sharp edges in the machined structures. As the voltage increases, the

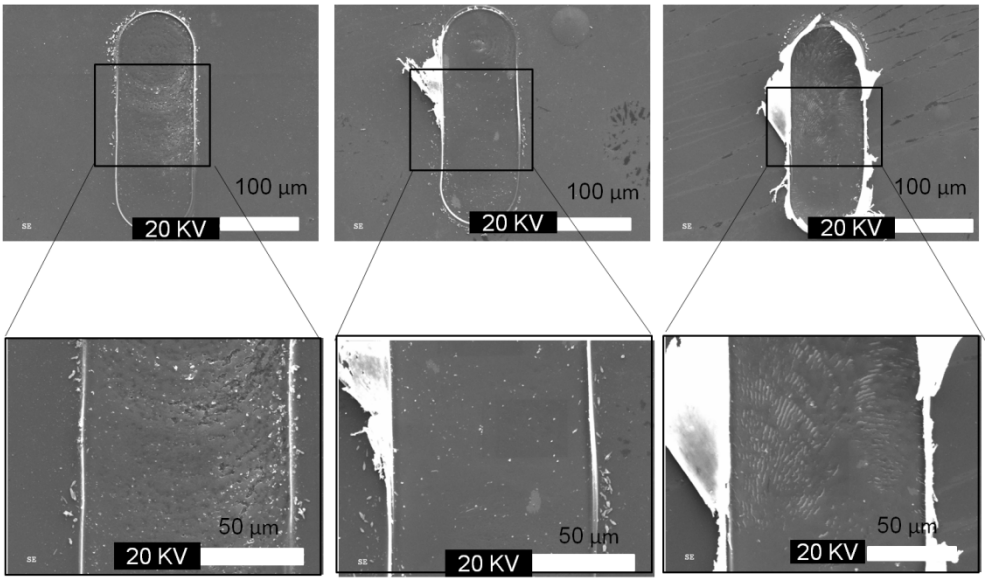

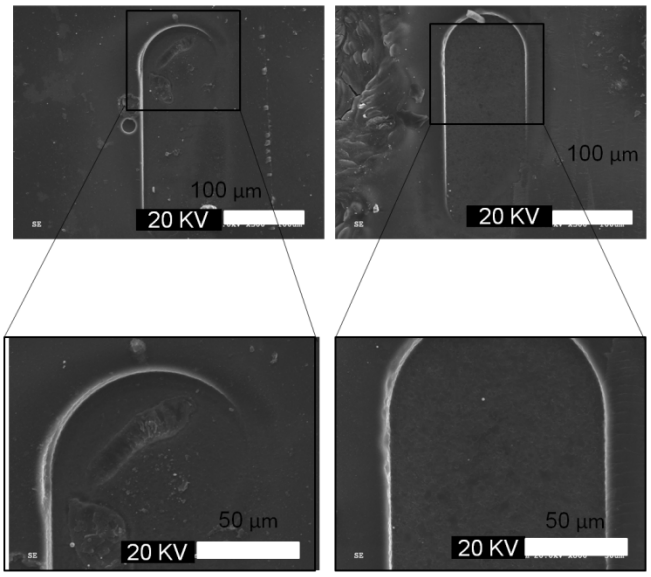

Fig. 3.5 SEM Images of Linear Structure with (a) 60 V-C_s (b) 60 V-10 pF (c) 60 V-100 pF (d) 80 V-C_s (e) 100 V-C_s

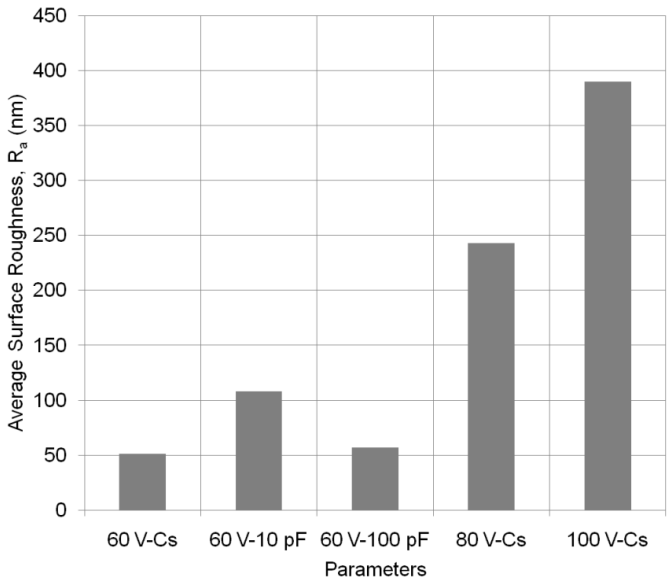

Fig. 3.6 Average Surface Roughness with Different Parameters

discharge gap can increase, and this condition might have enhanced heat dissipation by fluid flow and led to better discharge generation and EDM removal.

Average surface roughness was also measured across the width on the processed surfaces of the structures patterned using varying voltage-capacitance parameters (Fig. 3.6). It can be seen that similar roughness resulted with varying capacitances at 60 V. This result is, in fact, consistent with the hypothesis of mechanical scratching effect (due to thermal alteration of electrical conductivity) discussed earlier, which can lead to similar surface quality as EDM does not involve much if that is the case. However, there is steep increase in surface roughness with increasing voltage while using stray capacitance. This result also matches well with the above hypothesis for the cases with increased voltages, in which EDM removal dominates scratching effect and the surface roughness increases as the total energy rises with increase in voltage.

To quantify the average peak current of the discharge pulses, the current pulses were captured using the current probe (Fig. 2.6), and the data were processed to calculate the average value of

the peak current. The average peak current (I_{max}) was calculated (from ~130 of sampled pulses) Discharge currents were measured for different parameters as depicted in Fig. 3.7. It can be seen that the increases of the average peak current with increasing capacitances (C) at 60 V were smaller than what were theoretically expected due to the increases of the capacitance (C should be proportional to square of I_{max}). This may be due to the possibility of thermal alteration reducing the conductivity as discussed earlier, potentially suppressing the discharge current. In contrast, increasing the voltage (with C_s) resulted in steep rises of the current, with a trend very similar to that is seen in Fig. 3.6. This suggests that the result in the surface roughness is largely related to the amount of discharge current. It can also be seen that the current increases do not scale the voltage increases (they should be proportionally related). This could also be associated with the hypothesis in the polypyrrole's conductivity, in which discharge gap becomes smaller for smaller voltages leading to more hear accumulation and conductivity reduction consequently more reduction in the discharge current compared with the cases with larger voltages.

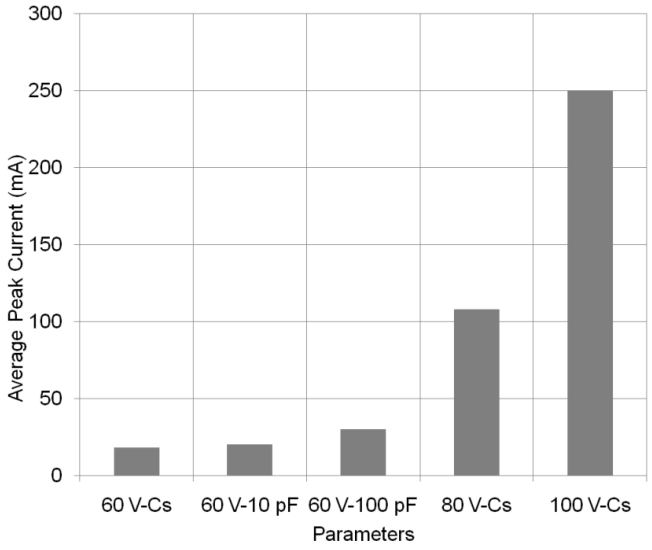

Fig. 3.7 Average Peak Current with Different Parameters

3.2.2 Scaling Effects

The previous study revealed that the condition of 60 V and stray capacitance (C_s) resulted in stable machining with the highest machining quality providing burr-free structures and the smallest surface roughness. Based on this result, the above voltage-capacitor combination was utilized as an optimal condition for the rest of experiments performed in this thesis. This section focuses on the scaling effects of the polypyrrole patterning under the EDM condition. To investigate the effect of electrode size on machining polypyrrole, the diameter of the tungsten electrode was reduced from 300 μm to 100 μm, 50 μm and 20 μm using WEDG. These tools were used to machine polypyrrole with the 60 V and C_s.

To investigate the effect of pattern size on the structures machined in polypyrrole, different square patterns were created by scanning the electrodes with different diameters in the X and Y directions while machining using the above discharge condition; the lengths of the side of the square pattern were defined to be 300 μm, 150 μm, and 60 μm for the electrodes with 100 μm, 50 μm, and 20 μm diameters.

The electrode was fed into the material with a 0.5-μm step along the Z direction. In this process, firstly 1.5 μm was machined using 0.5 μm step removal. Then 2.5 μm was machined using the same step removal and finally 3.5 μm was machined with same step removal, so that the total machined depth became 7.5 μm. This was done to ensure that there was no through hole on polypyrrole sheet and also to ensure that there is no mechanical scratching which was discussed in section 3.2.1. As performed before (Fig. 3.4), the position of Z-axis with time was recorded during the machining process. Fig. 3.8 shows the results for the last step of the sequence (for the removal depth of 3.5 μm), indicating stable removal processes without short circuiting in all the cases. It can also be seen from Fig. 3.8 that the machining time for this common depth decreased

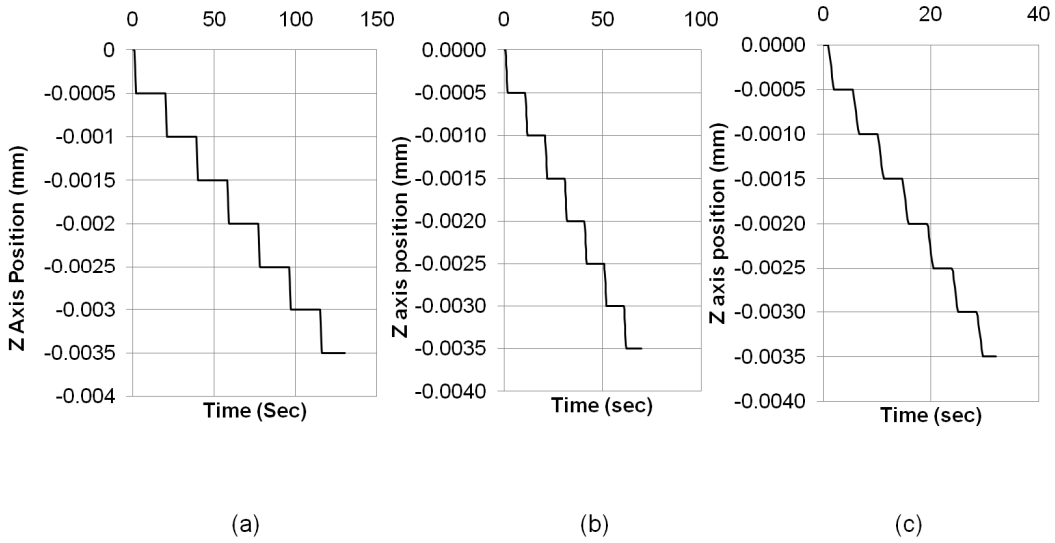

Fig. 3.8 Position of Z Axis with Machining Time for Rectangular Structure with (a) 100 μm (b) 50 μm (c) 20 μm Electrode

(from 132 s to 32 s) as smaller pattern/electrodes were involved. Fig. 3.9 shows obtained structures with the three patterns. It can be clearly seen from these images that μEDM is capable of producing fine patterns with sharp edges effectively. However, there is significant amount of debris as shown in Fig. 3.9 (a) compared to similar condition as described in Fig. 3.5(a). This may be attributed to the fact that the electrode scanned over a larger area in 3.9(a) compared to 3.5 (a). Therefore, if the polypyrrole sheet is not completely flat, there is possibility of reduced discharge gap in case of Fig. 3.5 (a) compared to Fig. 3.9 (a). Due to this reduced discharge gap, flushing of particles produced in the narrow gap is not sufficient. This debris may resolidified and adhere to the surface. Moreover, it is evident from the close-up images in Fig. 3.9 that some debris (particles) were left on the bottom surfaces patterned with the 100 μm and 50 μm electrodes, whereas the surface patterned with the 20 μm electrode was much cleaner than the

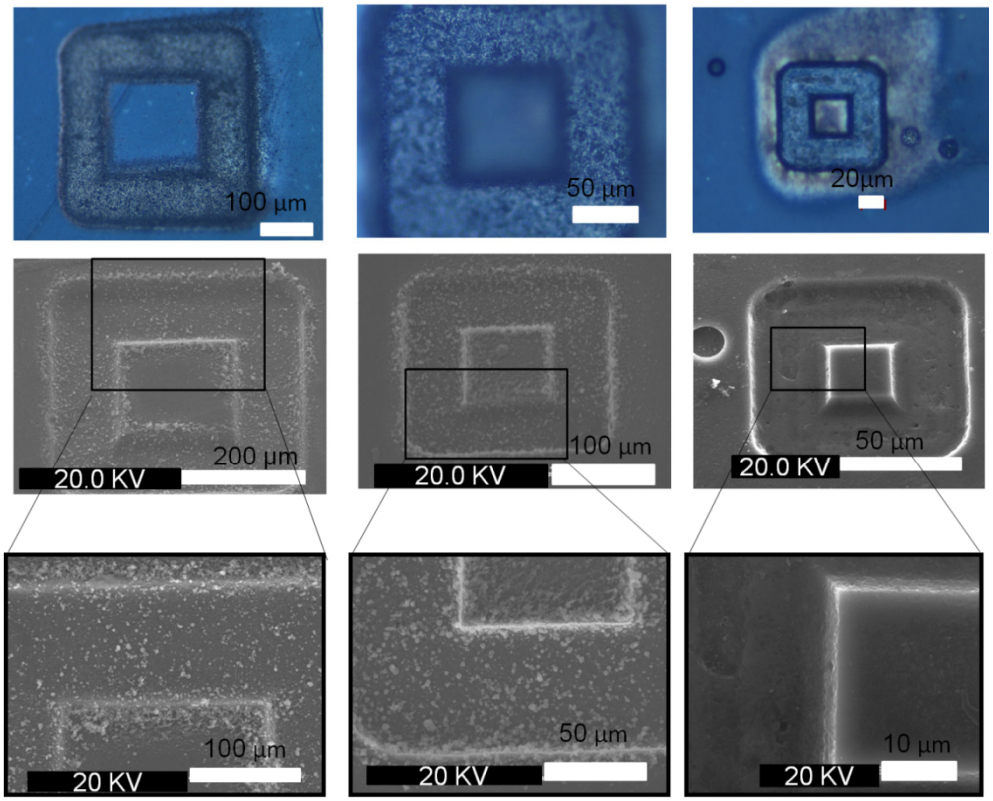

Fig. 3.9 Optical Microscope and SEM Images of Rectangular Structure of (a) 300 µm with 100 µm Electrode (b) 150 µm with 50 µm Electrode (c) 60 µm with 20 µm Electrode

other cases. Although the exact mechanism of this result is not clear, it might be attributed to a potential condition that flushing of particles produced in the narrow gap between the electrode's bottom and the sample surface occurs more effectively when smaller electrodes are used. In other words, thermally-induced fluidic forces that disperse melted particles may not be sufficient when the electrode's diameter is larger (than 20 µm in this experiment), and consequently the particles that remain in the gap may fully solidified and adhere to the patterned surfaces as observed.

The discharge gap, i.e., the clearance between the electrode and workpiece surfaces, represents the tolerance of μEDM. In the current experiments, this gap is approximately equivalent a half of the difference between the electrode diameter and the width of a patterned slot. Measuring this width in the images shown in Fig. 3.9 suggests that the three cases exhibited similar discharge gaps of around 4.5-6 μm.

Fig. 3.10 shows the depth measurement of the machined structure using stylus profilometer. It can be seen from Fig. 3.10 that with 100 μm electrode the actual machining depth was 10-15 μm, with 50 μm electrode it was 7.5- 11 μm and for 20 μm electrode the depth was 6.5 - 7 μm. The profiles show some level of slopes on the bottom surfaces; this may be related to the flexibility of the polypyrrole samples, which may have led to different flatness conditions for each sample between when held on the EDM system and when placed on the profilometer. However, these results indicate a clear trend of enhanced removal with larger electrodes, resulting in the patterns

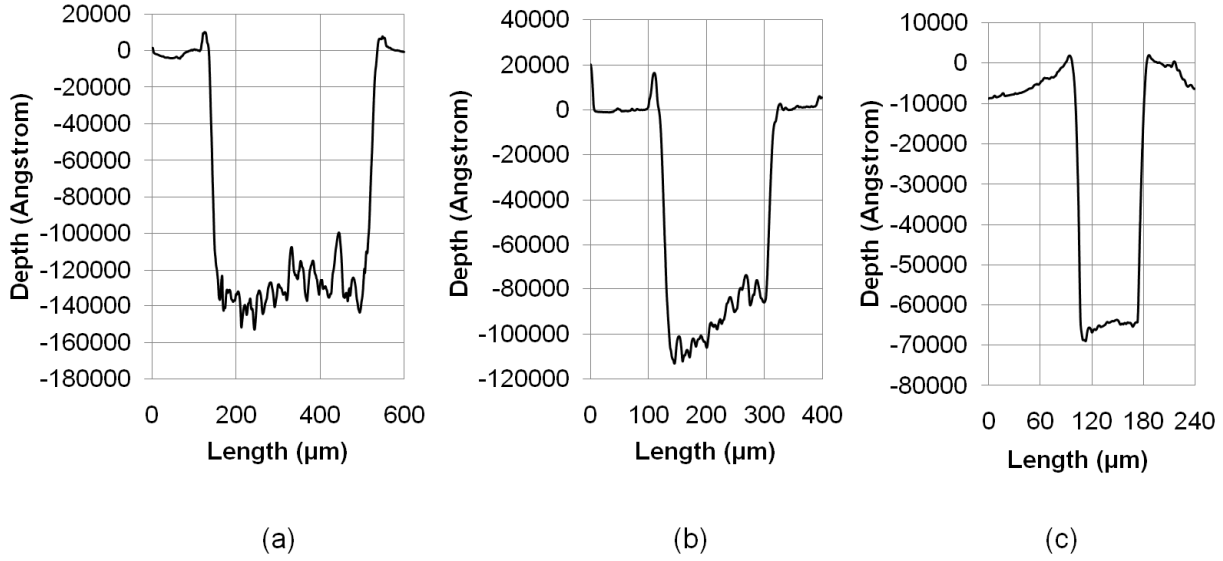

Fig. 3.10 Profile of Rectangular Structure of (a) 300 μm with 100 μm Electrode (b) 150 μm with 50 μm Electrode (c) 60 μm with 20 μm Electrode.

deeper than the programmed depth (of 7.5 μm). This outcome may be related to the presence of conductive particles (debris) produced in the gap; the conductive particles can weaken the dielectric breakdown strength of liquid and enhance discharge with more sparks [32].

Average surface roughness (R_a) of the patterned surface across their length was quantified using the profile data and plotted in Fig. 3.11. As indicated, there is a similar dependence of the roughness on the size of the electrode. For example, R_a of the surface created with the 20 μm electrode is ~10× smaller than the surface produced with the 100 μm electrode. This increased roughness with larger electrodes may be associated with the presence of the particles on the corresponding patterned surfaces. The hypothesis of resultant enhanced discharge noted above also supports the rougher surfaces in these cases.

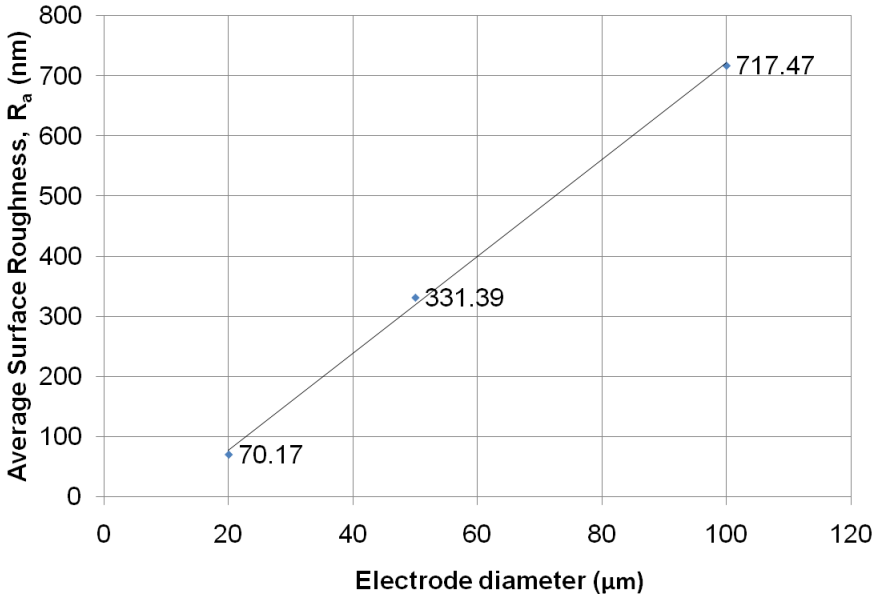

Fig. 3.11 Average Surface Roughness with Different Electrode Diameter

3.2.3 Discharge Current

3.2.3.1 Measurement Results

Average currents for 60 μm rectangular structures, patterned with 20 μm electrode using 60 V and stray capacitance (C_s), were measured by following the procedure described earlier. A sample waveform of the captured current pulses is shown in Fig. 3.12. The average peak current was calculated (from ~130 of sampled pulses) to be approximately 37 mA. From the same data, the average frequency of the generated pulses was measured to be 0.83 MHz. Although this frequency level is comparable to that typically seen in conventional μEDM, the average pulse current observed is much smaller than the current levels involved in the conventional process for metals (a few to several 100's mA, for the voltage and capacitor used in this test). This is likely attributed to the resistivity level of the polypyrrole that is three to four orders of magnitude larger than the levels of metals.

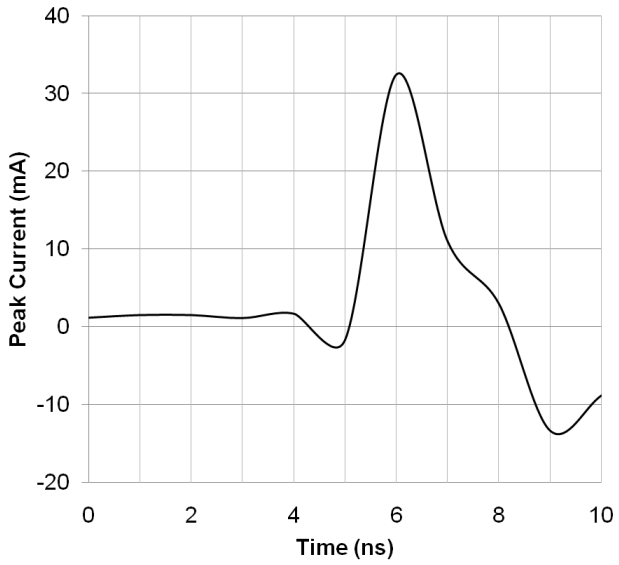

Fig. 3.12 Pulse Width and Peak Current Measurements Using 20 μm Diameter Electrode

As indicated in the above observation, the resistive characteristic of polypyrrole may affect the discharge current hence the removal process. This means that the machining process may also be affected by how the sample is electrically coupled with the discharge circuit, which in turn determines the paths for electrons to flow through the material during a discharge generation. To investigate this effect, three different modes of contact were tested using the same EDM condition (60 V with C_s). The first mode (Mode-1) was the setting same as the previous experiments, in which a sample was directly placed on the metallic base as shown in Fig. 3.13(a). In this case, the discharge current flows through the material vertically, i.e., the shortest distance for electrons to travel through the material which is the thickness of the material (20-30 μm). The second mode (Mode-2) was the setting in which an insulation layer was inserted between the sample and the base, and the electrical contact to the sample was made on top of the sample at a distance of 7.3 mm from the electrode, as shown in Fig. 3.13(b). This second setting forces the current to flow through the material laterally, for a distance much larger than the Mode-1 case. The third mode (Mode-3) setting was similar to second mode except the electrical contact to the sample was made on top of the sample at a distance of 3.5 mm from the electrode as shown in Fig. 3.13 (c). The third setting forces the current flow laterally similar to the second setting except the distance is smaller than the second setting. The average currents measured for these configurations are compared in Fig. 3.14. The current for Mode-3 was larger than that for Mode-2. This is directly related to the fact that the resistance between the electrode and the contact was smaller for Mode-3 than that for Mode-2 (measured to be 48 Ω vs. 88 Ω). This result suggests that for μEDM of a polypyrrole layer with the dielectric substrate, e.g., patterning the layer deposited on a medical catheter, the electrical contact to the layer with respect to the position of electrode will be an important factor for discharge generation.

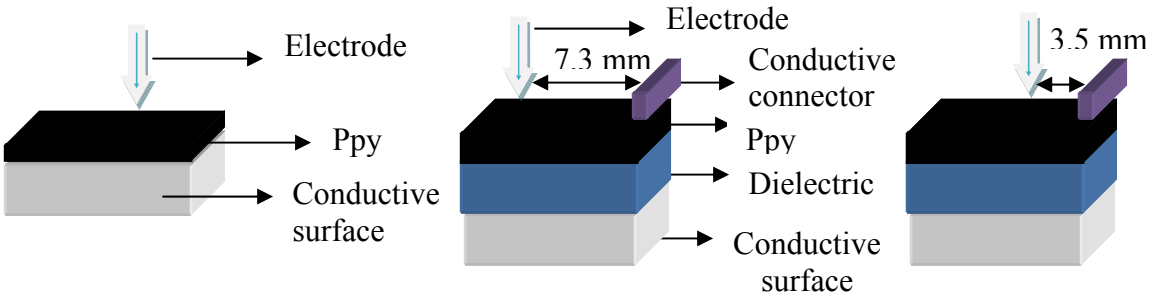

(a) (b) (c)

Fig. 3.13 Schematic of Different Contact Modes of Polypyrrole (a) Mode-1 (b) Mode-2 (c) Mode-3

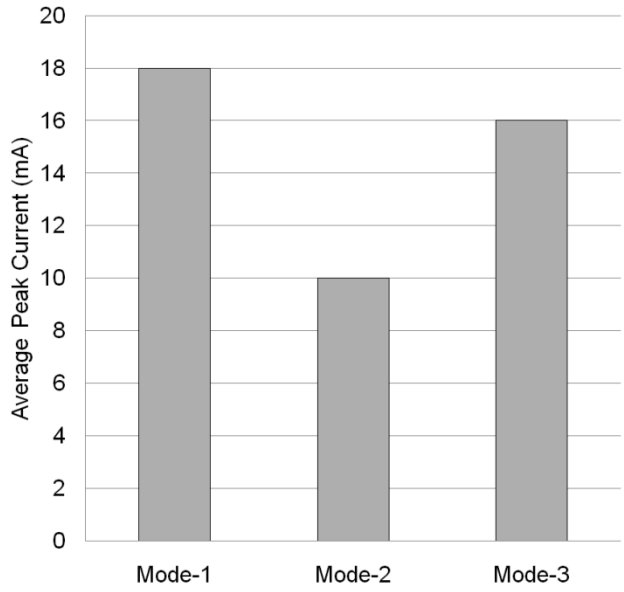

Fig. 3.14 Experimental Measurement of Current for (a) Mode-1 (b) Mode-2 (c) Mode-3

As shown in Fig. 3.14, the average current for Mode-1 in this experiment was measured to be 18 mA, close to the current level for Mode-3 (16 mA). The resistance between the electrode and the

base was measured to be 40 Ω in this setting, which is also close to that for Mode-3 and thus consistent with the result in the current. This relatively high resistance in Mode-1 may be due to a non-flatness of the sample (which was partly held by magnets), leading to non-uniform, and partial electrical contact on the backside of the sample. This is presumably a major reason that the current level is lower than the average current noted earlier (37 mA). The result here evidently suggests that for bare polypyrrole samples, the resultant discharge current can depend on the holding method for a particular sample.

3.2.3.2 SPICE Simulation

The discharge currents for the different modes of contact were simulated using LT SPICE. Fig. 3.15 shows the circuit model used to simulate the RC pulse generator involved in the μEDM experiments. The DC voltage supply V1 charges the capacitor C1 through the resistor R1. For the simulation purpose, a simple model comprised of a voltage-controlled switch S1 with a series-connected zener diode D1 was used to represent the discharge gap. A pulse voltage V2 turns on S1 to trigger a discharge of C1 to create a current pulse through the discharge circuit. The pulse frequency was set to be 16.67 MHz (assuming 60 ns pulse interval). The breakdown voltage of D1 is used to match the steady state arc voltage. The discharge gap of micro-EDM process is modeled according to the description in a previous study [17]. As discussed in this study, when the applied voltage between electrode and workpiece exceeds a threshold voltage, breakdown is triggered. The voltage instantly drops to a constant arc voltage that is sustained during the discharge. When the current supplied from the capacitor diminished, this arc ends. In the current modeling, the breakdown voltage of D1 was set to 15 V for V1 of 60 V by scaling the arc voltage reported for a discharge voltage of 80 V [17]. The resistance R2 is a measured resistance of a polypyrrole film sample that is coupled with the discharge circuit in series.

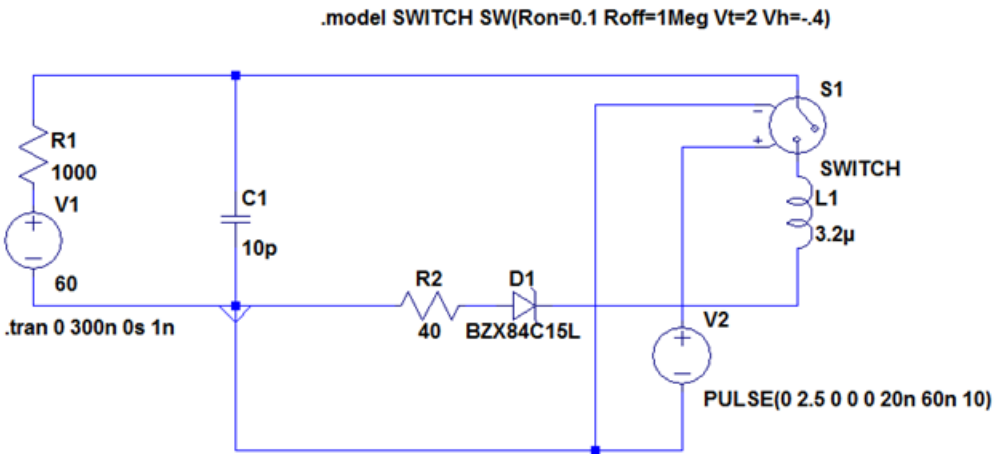

Fig. 3.15 LT SPICE Circuit Used for Simulation of Mode-1

An inductor L1 is also connected in series to represent a parasitic inductance of the actual circuit. The inductance was measured with a RLC meter and its value was 3.2 µH. This inductance causes the current to rise as a ramp. Fig. 3.15 shows R2 of 40 Ω, the polypyrrole resistance measured for Mode-1. The value of R2 was replaced with the corresponding measured value to simulate the other modes (Mode-2, Mode-3).The simulation results for Mode-1 case are depicted in Fig. 3.16. Discharge currents through R2 and C1 are denoted by I (R2) and I (C1) respectively. Pulse duration to turn on S1 was set to 20 ns as denoted by duration of V (n002). Fig. 3.17 shows the variation of the simulation result of peak current for three modes of contact. It can be seen that the trend of current with varying resistance is similar to the experimental results. The peak current of the pulses through R2 is observed to reach around 84 mA for Mode-1. The average peak current observed in the experiment for Mode-1 was 18 mA (Fig. 3.14). The deviation observed in the simulation results may be due to the fact that during the measurement of resistance of the polypyrrole film, pressing the tip of the probes of the multimeter may have resulted in much larger contact areas than the area of actual discharge point. This condition may

lead to smaller resistance and thus larger currents in the simulation. Moreover, the actual values of resistance of polypyrrole film during experiments in different modes of contact may be higher than measured values due to the hypothetical condition of thermal dependence of electrical conductivity of polypyrrole discussed earlier. This effect can also results in larger currents in simulation.

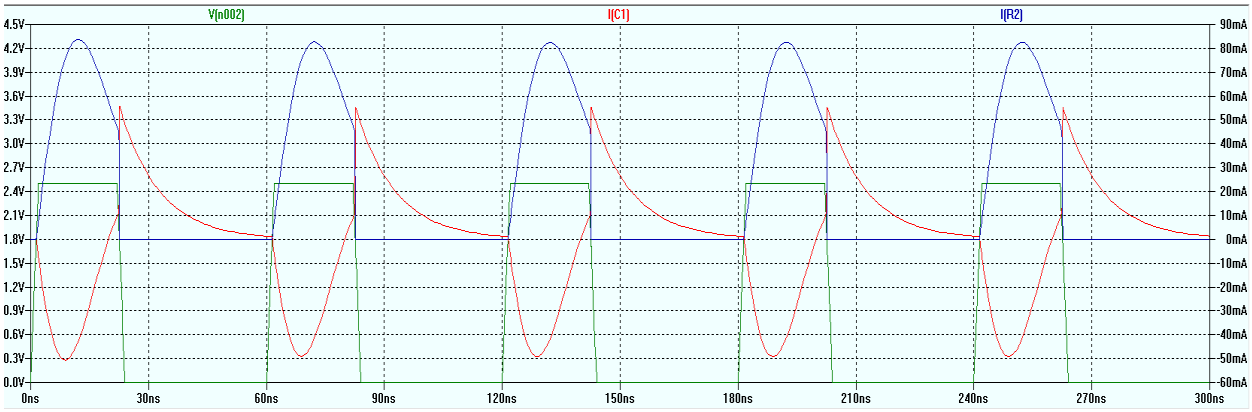

Fig. 3.16 LT SPICE Simulation Result for Current and Voltage of Mode-1

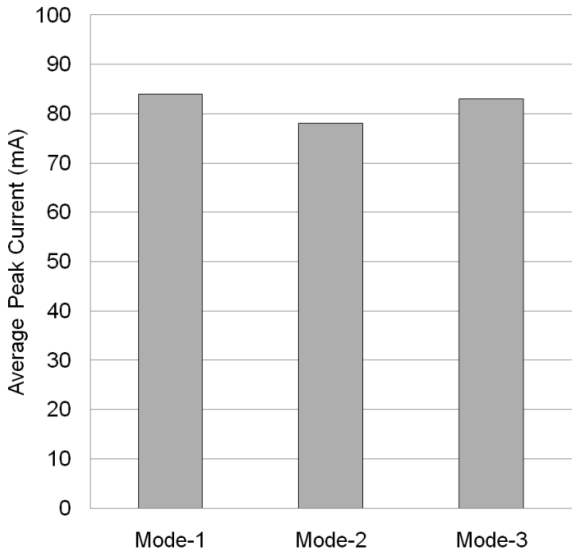

Fig. 3.17 Graphical Representation of Simulation Results of Current

3.2.4 Generation of Single Discharge and Analysis

In μEDM, the erosion takes place through a series of discharge sparks generated between the electrode and the workpiece. Therefore, it is important to characterize the effect of single discharge on the removal of the material (polypyrrole in this study). For this study, an RC circuit shown in Fig. 3.18 was prepared in a bread board. The circuit used a 1 KΩ resistance, a 3.30 nF capacitance and two switches and was coupled with a DC power supply of 120 V as shown. The setting of 3.30 nF and 120 V is the maximum levels available in the μEDM system used, which was selected to emphasize the effect of the discharge and ease the analysis. This circuit was connected with electrode and workpiece holder of EDM machine as illustrated on Fig. 3.18. The diameter of the electrode used in this study was 100 μm. In the initial state, switch 1 is turned on, switch 2 is turned off and electrode is far away from the workpiece. With this, the capacitor is fully charged through the resistor and switch 1 but cannot discharge through switch 2. In the next phase, switch 1 is turned off, switch 2 is turned on and then the electrode is fed in Z direction toward the workpiece until a spark is detected. This allows the capacitor to discharge, creating a single spark between electrode and workpiece, but does not allow charging to it as switch 1 is off. Therefore, no subsequent spark occurs after the first one.

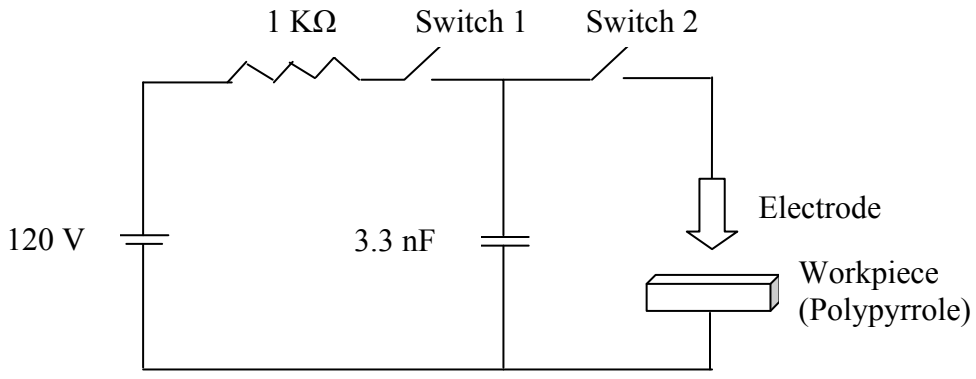

Fig. 3.18 Set-Up for Single Discharge Experiment

This experiment was conducted in polypyrrole as well as stainless steel (SU 304) for comparison. Fig. 3.19 shows the SEM images of several different crater marks created by single spark discharges on polypyrrole (Figs. 3.19(a) - (f)) and created on stainless steel (Fig. 3.19(g)). It can be observed that the craters created on polypyrrole were not uniform and round when compared to stainless steel. This could be attributed to the fact that stainless steel has higher thermal conductivity compared to polypyrrole. Therefore, heat, generated during μEDM, conducted through stainless steel more quickly compared to conduction through polypyrrole. As a result, size of the crater is smaller compared to polypyrrole. The difference in the crater shapes between the polypyrrole and stainless steel may be related to the difference in their removal modes- In stainless steel, a spark locally melts it and surface tensions of the molted portion might make the crater shape more round during its cooling cycle, whereas, polypyrrole may be directly vaporized by a spark (without forming liquid) in which there is no surface tension effect, resulting in more random shapes compared with the stainless steel case. Further, to observe the effect of multiple single sparks on material composition, a double spark was created on polypyrrole. The resultant crater produced is shown in Fig. 3.20 (a). It can be observed that the size of craters increased compared with the single case and the pattern became more uniform and round shape.

To analyze the effect of discharge on the elemental composition of the material, EDX was performed for the crater shown in Fig. 3.20 (b) at four different regions (A) outside area (as a reference), (B) large island present at the center of the crater, (C) small islands (that look like grains with potentially resolidified debris), and (D) spaces between the grains. EDX of the same sample was also performed before submerging to EDM oil (i.e., dry state) which is denoted by "O". This was performed to observe the effect of EDM oil on polypyrrole.

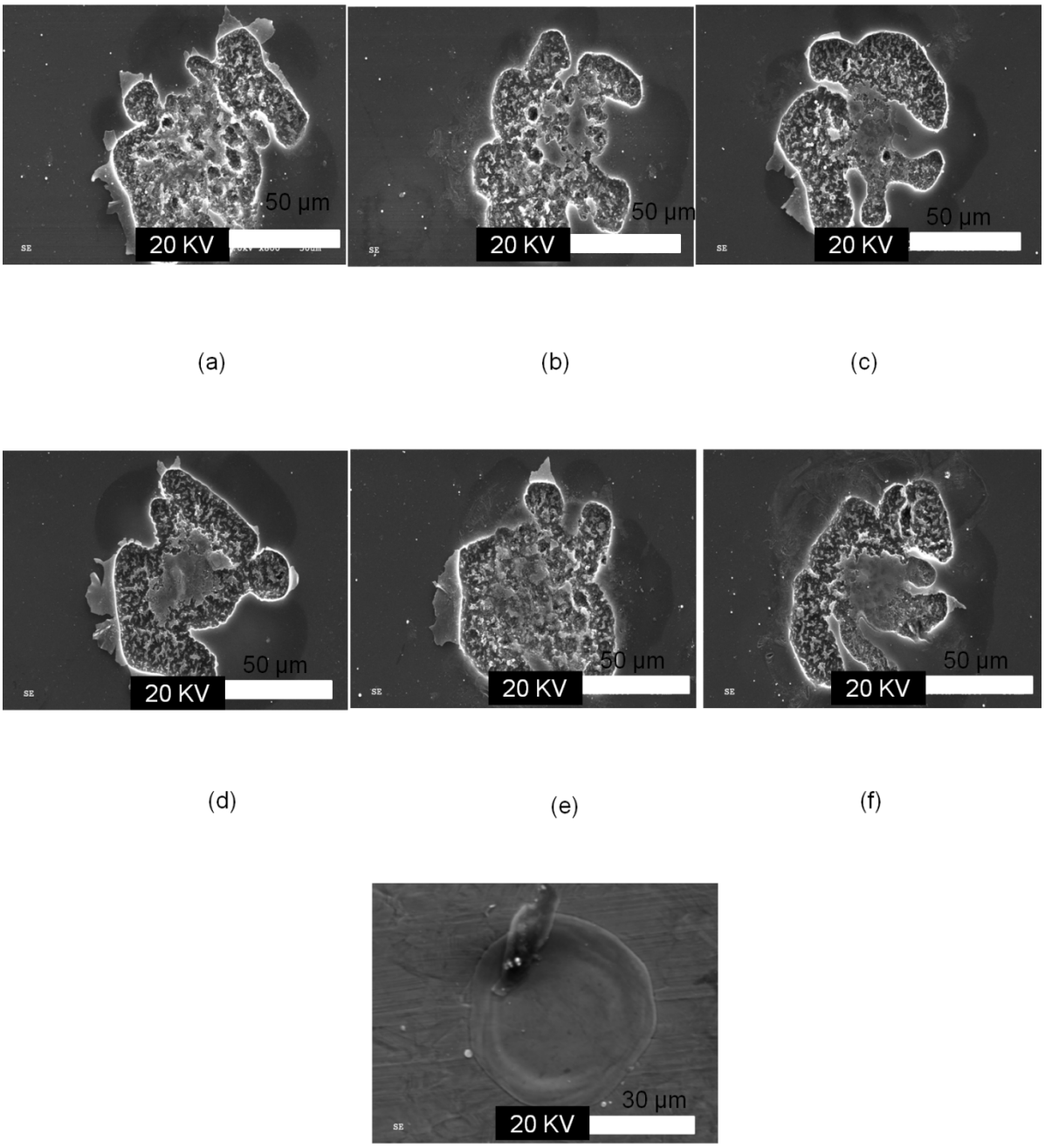

Fig. 3.19 SEM Images of Single Discharge Experiment on (a-f) Polypyrrole (g) Stainless Steel (SU 304)

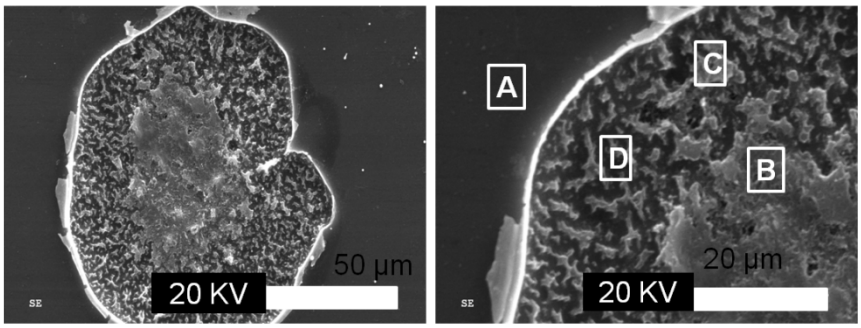

(a) (b)

Fig. 3.20 SEM Images of Double Discharge Experiment (a) Whole Area (b) Magnified Image with Different Areas Marked for EDX

Table 3.2: EDX Results on Double Discharge Area

Elements	**O**	**A**	**B**	**C**	**D**
Carbon	**41.99 wt%**	**42.19 wt%**	**43.03 wt%**	**48.37 wt%**	**47.37 wt%**
Nitrogen	16.94 wt%	16.98 wt%	18.19 wt%	17.07 wt%	15.62 wt%
Oxygen	**25.22 wt%**	**25.38 wt%**	**23.24 wt%**	**19.86 wt%**	**20.40 wt%**
Fluorine	2.63 wt%	2.29 wt%	2.65 wt%	1.74 wt%	1.63 wt%
Phosphorus	11.24 wt%	11.26 wt%	11.14 wt%	11.12 wt%	13.03 wt%
Copper	0.86 wt%	0.77 wt%	0.87 wt%	0.97 wt%	1.02 wt%

The major elements of EDX results are shown in Table 3.2. It can be observed from a comparison between “O” and “A” that submerging in the EDM oil itself did not cause significant

changes in the composition of polypyrrole. The results also indicate that overall, the percentage of carbon tends to be slightly higher (from 42.4% in A to 46.3%, the average of B, C and D) and that of oxygen to be slightly lower (from 25.4% in A to 21.2%, the average of B, C and D) after EDM. The carbon may have been added due to thermal decomposition of EDM oil that produces carbon residues. The reduction of oxygen may also be related to pyrolytic chemical reactions induced by discharge. Tungsten (electrode material) was detected in case of dry EDM (with air) as shown in Table 3.1; however, this is not the case for this wet μEDM in oil in which no detectable tungsten was observed – this is another favorable result that justifies the application of wet μEDM in oil for polypyrrole patterning.

3.3 Application: Polypyrrole Patterning toward Fabrication of Active Catheters

As discussed earlier, the application of polypyrrole actuators to active catheter devices is promising. To fabricate such catheters, polypyrrole is deposited on catheter to act as active element for catheter actuation and bending. As discussed in Section 2.2.2, polypyrrole is deposited on catheter using electroless followed by electrochemical deposition. This polypyrrole is then patterned to create electrically isolated electrodes. This patterning may be done using laser machining; however, the process tends to cause thermal damages and involves the need for complex system while being limited to serial processing as mentioned in section 1.1. If this patterning on the catheter is possible with μEDM, it can eliminate the issue involved with laser machining.

To conduct pattering with μEDM, catheter coated with polypyrrole was placed on a metallic V-groove slot. This V-groove was placed on workpiece holder of EDM machine. Two connectors

were added on both side of the catheter over the V-groove in order to mechanically hold the catheter on slots and also to provide good electrical contact through the V-groove. The film of polypyrrole deposited on the catheter is electrically coupled with the circuit through longitudinal surfaces that made contact with the V-groove surfaces. For experimental evaluation, a 3 mm slot was created on catheter by removing polypyrrole deposited on catheter using μEDM milling with 300 μm diameter tungsten electrode. The depth of the slot was kept greater than 60 μm even though the depth of polypyrrole deposition is around 10 μm. This was done to compensate the variation of depth due to vertical alignment of EDM workpiece holder and V-groove. Moreover, the wall thickness of catheter is around 330 μm. So even there is possibility of mechanical contact between electrode and catheter in certain areas, it will not eventually make through holes inside the catheter. The polypyrrole deposited on catheter was measured to have a contact resistance of 20.75 KΩ, much larger than the case for direct contact through the base observed (to be around 40 Ω) in the experiment discussed in Section 3.2.3.1. Therefore, higher energy is required to pattern polypyrrole deposited on catheter; the parameters of 120 V and 213.3 pF were able to remove polypyrrole from the catheter. Fig. 3.21 shows the patterned area. It can be seen from SEM image, that the patterned area is linear. The width of the patterned area is around 200 μm, smaller than the electrode diameter (300 μm), due to the curvature of the catheter that probably limited the actual width on which discharge pulses were generated. Moreover, there are some marks of mechanical contact on the exposed catheter surfaces due to higher removal depth. Similar patterning was performed on the other side of the catheter to create two isolated electrodes on the catheter. The resistance between the two electrodes was measured to be 5 MΩ. This indicates that the μEDM patterning is effective to make electrical isolation in polypyrrole films and to create isolated electrodes for the catheter application.

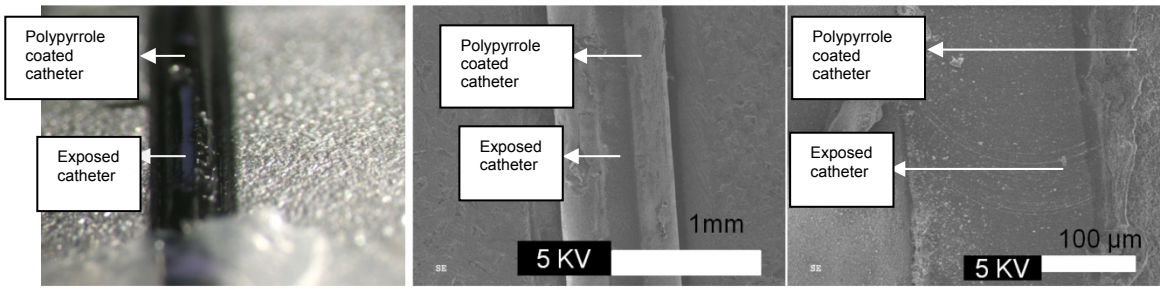

Fig. 3.21 Images of Patterned Polypyrrole on Catheter (a) Nikon Camera Image (b) SEM Images along the Length (c) Magnified Image of the Slot Width

For catheter actuation, a certain length of the catheter is required. To fabricate actual devices, it may need to pattern for the length of 25 mm. However, machining of 25 mm in one process is very slow and need to use even larger machining depths to compensate the total vertical misalignment along this length (which may increase damages to the catheter body due to mechanical removal). Therefore, in this preliminary experiment, milling length of 10 mm was used. After milling 10 mm with µEDM, the electrode was rotated to pattern the other side. Thus two electrodes of polypyrrole were created on the surface of catheter that was isolated from each other. Fig. 3.22 shows the SEM images of portion of both sides of the catheter and it depicts successful linear isolation of polypyrrole on both sides of the catheter. This catheter was used to evaluate if the electrodes created were effective to enable actuation of the catheter. An aqueous solution of $NaPF_6$ was used to actuate this 10 mm long catheter. The catheter was submerged in the solution using a clamp. The actuation potential was a step voltage of ±8 V across the two polymer electrodes. The half-cell potential between each polymer electrode and an Ag/AgCl reference electrode was measured during actuation to alternate between -4 V and +4 V. The actuation of catheter was monitored as depicted in Fig. 3.23.

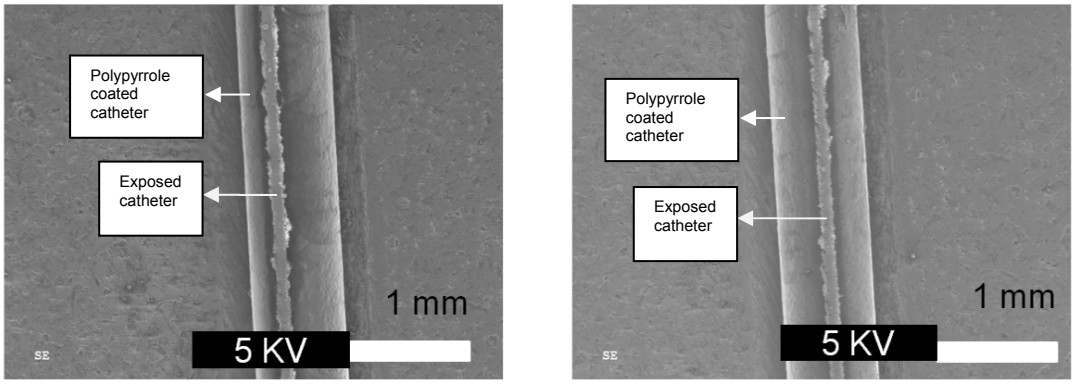

(a) (b)

Fig. 3.22 SEM Images of Portion of 10 mm Patterned Polypyrrole on Catheter (a) Before Rotation (b) After Rotation

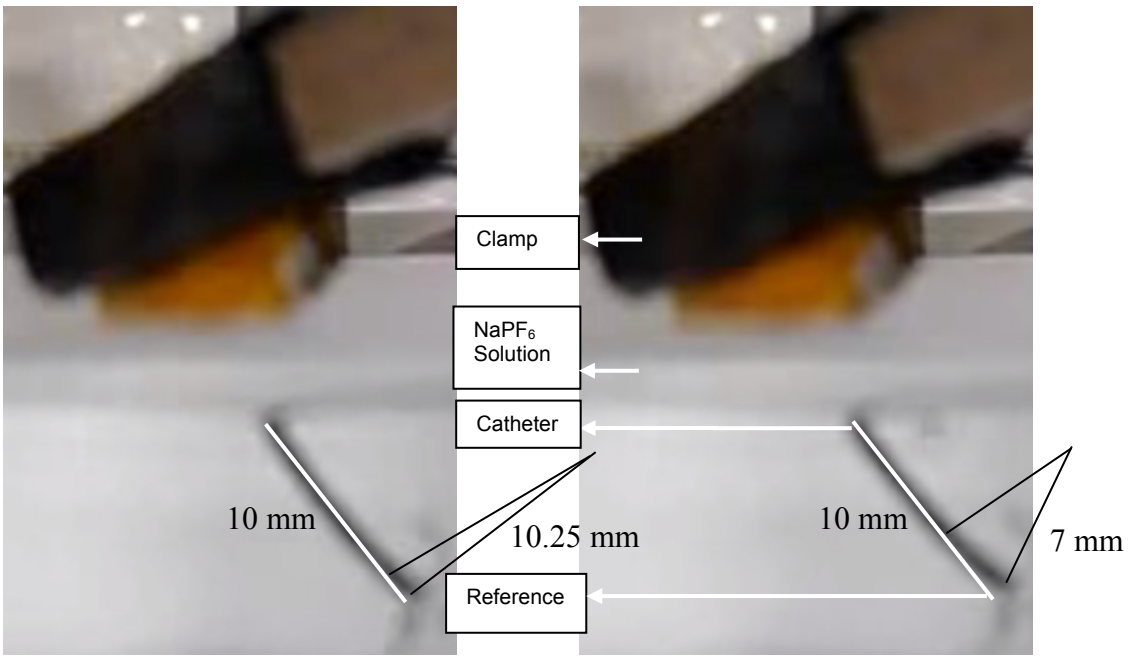

(a) (b)

Fig. 3.23 Images of Catheter (a) Before Actuation (b) After Actuation

The length of the catheter was approximately 10 mm. The length of the catheter is marked by white line in Fig. 3.23 which is considered as the reference line. The change of position of catheter with respect to reference line demonstrated actuation and bending of catheter. Before actuation, the radius of curvature was approximated to be 10.25 mm with respect to the reference line as shown in Fig. 3.23 (a). After actuation, the radius of curvature was reduced to approximately 7 mm as shown in Fig. 3.23 (b). This result verifies that the developed μEDM patterning process is effective for the fabrication of polypyrrole actuator and promising for the active catheter application. There have been reports of actuating catheter with much lower step voltage (±0.8 V) with bending radius of 9.8 mm [52]. With the present set-up, the contact resistance between the catheter and the clamp was high, leading to the requirement of high step voltage for actuation. Therefore, further optimization of the set up is necessary for catheter actuation with low voltage.

Chapter 4

Conclusions and Future Work

This study has investigated the feasibility of μEDM for micro-patterning of polypyrrole. It was experimentally shown that dry μEDM was able to create micro-holes and micro-structures using air as dielectric medium. However, in this case, patterned structures exhibited surface damages including micro-cracks in both drilling and milling processed structures. Moreover, EDX results showed that there was presence of electrode material on the surface of polypyrrole processed in air. It was experimentally shown that stable, high-precision micro-machining of the material could be performed using wet μEDM in commercially available EDM oil instead of dry μEDM in air. Parametric evaluation with varying voltages and capacitances in oil were conducted. There were signs of mechanical scratching rather than EDM removal at lower voltages. This observation was discussed with a hypothesis that discharge generation and currents were affected by thermal modification of electrical conductivity of polypyrrole. This hypothesis was observed to be consistent with various experimental observations. It was shown that processing at a discharge voltage of 60 V without an external capacitor, used for the RC pulse generation circuit, was observed to be an optimal machining condition with lowest average surface roughness (51 nm) and peak discharge current (18 mA). Differently sized micro-patterns were successfully created with depth control using tungsten electrodes with diameters ranging from 300 μm down to 20 μm. Micro-patterning of 60×60 μm^2 square shape with a controlled depth of 7.5 μm was demonstrated using a 20 μm diameter electrode. The generated discharge pulses exhibited an

average peak current of 37 mA and a pulse frequency of 0.83 MHz and resulted in discharge gaps of 4.5-6 μm. An experiment, that defined different electrical contacts made to polypyrrole samples, indicated that the distance between the electrode location and the terminal of the discharge circuit of the system, with which polypyrrole samples were coupled, was an important factor that determined the level of resultant discharge current. SPICE simulations were also conducted to analyze the peak current under different conditions in the electrical contact made to polypyrrole samples, showing a trend similar to the experimental results with deviation in their magnitudes; potential causes of this deviation were also discussed. A circuit was developed to observe the effect of single spark discharges of μEDM on polypyrrole and stainless steel for comparison. The results indicated that different removal modes of μEDM were involved for processing polypyrrole and stainless steel. EDX results indicated that EDM oil did not significantly affect the composition of polypyrrole. Even after μEDM processing with the highest level of the discharge energy, the composition of polypyrrole was observed to be still consistent. Polypyrrole deposited on medical catheters was also patterned using μEDM to create the electrodes of polypyrrole electrically isolated from each other. SEM images and electrical measurement showed that the process was effective to create electrical isolation with very high resistance (~5 MΩ) between the electrodes. These polypyrrole electrodes patterned on the catheter were used as a mechanically active element for catheter actuation. The actuation of the catheter, with radius of curvature of ~ 7 mm, was successfully demonstrated at a step voltage of ±8 V across the two patterned electrodes. The actuation voltage was high and suggests the need for further optimization of the set-up.

The developed μEDM technique is potentially much more straightforward to control and cost-effective compared with other reported techniques for polypyrrole micro-machining such as laser

machining and lithography-based processes. The obtained results suggest that μEDM can be an alternative method for polypyrrole micro-patterning that may broadly expand application opportunities for this material, encouraging further studies of not only polypyrrole μEDM toward higher precision and higher throughput but also the application to other conducting polymers. Toward this end, following extended studies and developments are recommended as:

- To grow polypyrrole on a solid substrate and conduct experiments on polypyrrole grown on soild substrate in order to eliminate the issue of flatness.
- μEDM is relatively slow in terms of processing polypyrrole. Therefore it is necessary to investigate the feasibility of batch mode μEDM to pattern polypyrrole.
- The flushing medium should be pressure controlled to ensure proper removal of debris from the gap which may be beneficial to control depth of removal.
- The V-groove to hold the catheter should be designed such a way that it can be adjusted to eliminate the issue of flatness that can reduce the machining depth.
- Actuation voltage of catheter should be optimized further.
- The feasibility of using μEDM to pattern other conducting polymers such as Polyaniline and Poly (3,4-ethylenedioxythiophene) (PEDOT) should be investigated.

References

[1] T. A. Skotheim, *Handbook of conducting polymers*, vol. 1, Newyork: Marcel Dekker Inc., 1986.

[2] J. D. Madden, P. G. Madden, I. W. Hunter, "Conducting polymer actuators as engineering materials," *Proceedings of SPIE, Smart Structures and Materials 2002: Electroactive Polymer Actuators and Devices (EAPAD)*, 4695(1), pp. 176-190, 2002.

[3] M. Angelopoulos, "Conducting polymers in microelectronics," *IBM J. Res. & Dev*., 45(1), pp. 57-75, 2001.

[4] J. D. W. Madden, N. A. Vandesteeg, P. A. Anquetil, P. G. A. Madden, A. Takshi, R. Z. Pytel, " Artificial muscle technology: Physical principles and naval prospects," *IEEE Journal of Oceanic Engineering*, 29(3), pp.706-728, 2004.

[5] A. Mazzoldi, D. De Rossi, "Conductive polymer based structures for a steerable catheter," Smart Structures and Materials 2000: Electroactive Polymer Actuators and Devices (EAPAD), 3987, pp. 273-280, 2000.

[6] D. K. Yfantis, A. D. Yfantis, S. Lamprakopoulos, S. Depountis, C. D. Yfantis , D. Schmeisser, "New environmentally friendly methods – composite coatings based on polypyrroles," *WSEAS Transactions on Environment and Development*, 2(3), pp.167-172, 2006.

[7] J. D. W. Madden, B. Schmid, M. Hechinger, S. R. Lafontaine, P. G. A. Madden, F. S. Hover, "Application of polypyrrole actuators: Feasibility of variable camber foils," *IEEE Journal of Oceanic Engineering*, 29(3), pp. 738-749, 2004.

[8] T. Shoa, N. R. Munce, V. Yang, J. D. Madden, "Conducting polymer actuator driven catheter: Overview and applications," *Proc. of SPIE, Electroactive Polymer Actuators and Devices (EAPAD),* 7287(1), pp. 72871J1- 72871J9, 2009.

[9] A. D. Santa, A. Mazzoldi, D. De Rossi, "Steerable microcatheters actuated by embedded conducting polymer structures," *Journal of Intelligent Material Systems and Structures*, 7(3), pp.292-300, 1996.

[10] A.D. Santa, D. De Rossi, "Intravascular microcatheters steered by conducting polymer actuators," Engineering in Medicine and Biology Society, Bridging Disciplines for Biomedicine, Proceedings of the 18th Annual International Conference of the IEEE, 5, pp. 2203-2204, 1996.

[11] A. Ramanaviciene, A. Ramanavicius, "Application of polypyrrole for the creation of immunosensors," *Critical Reviews in Analytical Chemistry*, 32(3), pp. 245-252, 2002.

[12] E. W. H. Jager, E. Smela, O. Inganäs, "Microfabricating conjugated polymer actuators," *Science*, 290(5496), pp. 1540-1545, 2000.

[13] A. Nannini, G. Serra, "Growth of polypyrrole in a pattern: A technological approach to conducting polymers," *J. Mol. Electron.*, 6, pp. 81-88, 1990.

[14] D.M. Collard, C.N. Sayre, "Micron-scale patterning of conjugated polymers on microcontact printed patterns of self-assembled monolayers," *Synthetic Metals,* 84(1–3), pp. 329-332, 1997.

[15] K.K.C. Lee, N.R. Munce, T. Shoa, L. G. Charron, G.A. Wright, J.D. Madden, "Fabrication and characterization of laser-micromachined polypyrrole-based artificial muscle actuated catheters," *Sensors and Actuators A: Physical*, 153(2), pp. 230-236, 2009.

[16] N.H. Rizvi, "Femtosecond laser micromachining: Current status and applications," *RIKEN Review no. 50: Focused on Laser Precision Micro Fabrication (LPM 2002)*, pp. 107-112, 2003.

[17] K. Takahata, Y.B. Gianchandani, "Batch mode micro-EDM for high-density and high-throughput micromachining," *The 14th IEEE International Conference on Micro Electro Mechanical Systems(MEMS)*, pp. 72-75, 2001.

[18] J.D. Madden, T.S. Kanigan, S. Lafontaine, I.W. Hunter, "Conducting polymer actuator." US Patent 6,249,076 B1, June 19, 2001.

[19] K.P. Rajurkar, Z.Y. Yu, "3D micro-EDM using CAD/CAM," *CIRP Annals - Manufacturing Technology*, 49(1), pp. 127-130, 2000.

[20] K.P. Rajurkar, G. Levy, A. Malshe, M.M. Sundaram, J. McGeough, X. Hu, "Micro and nano machining by electro-physical and chemical processes," *CIRP Annals - Manufacturing Technology,* 55(2), pp. 643-666, 2006.

[21] S. Kalpajian, S.R. Schmid, "Material removal processes: Abrasive, chemical, electrical and high-energy beam," in *Manufacturing processes for engineering materials*, Ed. New Jersey: Prentice Hall, 2003, pp. 541.

[22] S. Webzell, "That first step into EDM," in *Machinery*, 159 (4040), Ed. Kent, UK: Findlay Publications Ltd., 2001, pp. 41.

[23] E.C. Jameson, *Electrical discharge machining,* Dearbern, Michigan: Society of Manufacturing Engineers, 2001, pp. 12.

[24] L. Houman, "Total EDM," in *Electrical discharge machining: Tooling, methods and applications*, E. C. Jameson, Ed. Dearbern, Michigan: Society of Manufacturing Engineers, 1983, pp. 5-19.

[25] H. Kurafuji, T. Masuzawa, "Micro-EDM of cemented carbide alloys," *Jpn Soc Electr Mach Eng.,* 2(3), pp. 1-16, 1968.

[26] M.P. Jahan, A. B. M. A. Asad, M. Rahman, Y.S. Wong, T. Masaki, "Micro-electro discharge machining (μEDM)," in *Micro-manufacturing: Design and manufacturing of micro-products* , 1st ed., M. Koc, T. Ozel, Ed. John Wiley & Sons, Inc, 2011, pp. 301-347.

[27] L. Llanes, E. Idanez, , E. Martinez, B. Casas, J. Esteve, "Influence of electrical discharge machining on the sliding contact response of cemented carbides," *International Journal of Refractory Metals and Hard Materials,*19(1), pp. 35-40, 2001.

[28] D.M. Allen, A. Lecheheb, "Micro electro-discharge machining of ink jet nozzles: Optimum selection of material and machining parameters," *Journal of Materials Processing Technology,* 58(1), pp. 53-66, 1996.

[29] E.B. Guitrau, *The EDM handbook*, Cincinnati: Hanser Gardner Publications, 1997.

[30] T. Masuzawa, "State of the art of micromachining," *CIRP Annals - Manufacturing Technology,* 49(2), pp. 473-488, 2000.

[31] B.M. Schumacher, "After 60 years of EDM the discharge process remains still disputed," *Journal of Materials Processing Technology,* 149(1–3), pp. 376-381, 2004.

[32] M. Kunieda, B. Lauwers, K.P. Rajurkar, B.M. Schumacher, "Advancing EDM through fundamental insight into the process," *CIRP Annals - Manufacturing Technology,* 54(2), pp. 64-87, 2005.

[33] F. Han, S. Wachi, M. Kunieda, "Improvement of machining characteristics of micro-EDM using transistor type isopulse generator and servo feed control," *Precision Engineering,* 28(4), pp. 378-385, 2004.

[34] M. Kunieda, "Challenges to miniaturization in micro-EDM," *ASPE Proceedings of Annual Meeting 23,* 2008.

[35] T. Masaki, K. Kawata, T. Masuzawa, "Micro electro-discharge machining and its applications," *Micro Electro Mechanical Systems, Proceedings, an Investigation of Micro Structures, Sensors, Actuators, Machines and Robots, IEEE,* pp. 21-26, 1990.

[36] M. Rahman, A. B. M. A. Asad, T. Masaki, Y.S. Wong, H. S. Lim, "Integrated hybrid Micro/Nano-machining," *ASME Conference Proceedings,* 42908, pp.197-209, 2007.

[37] T. Masuzawa, H.K. Tönshoff, "Three-dimensional micromachining by machine tools," *CIRP Annals - Manufacturing Technology,* 46(2), pp. 621-628, 1997.

[38] K. Egashira, K. Mizutani, "EDM at low open-circuit voltage," *Journal of the Japan Society of Electrical Machining Engineers,* 10, pp. 21-26, 2005.

[39] F. Han, Y. Yamada, T. Kawakami, M. Kunieda, "Investigations on feasibility of submicrometer order manufacturing using micro-EDM," *ASPE, Annual Meeting, 30,* pp. 551-554, 2003.

[40] A.P. .Malshe, K. Virwani, K.P. Rajurkar, D. Deshpande, "Investigation of nanoscale electro machining (nano-EM) in dielectric oil," *CIRP Annals - Manufacturing Technology,* 54(1), pp. 175-178, 2005.

[41] J. Murray, D. Zdebski, A.T. Clare, "Workpiece debris deposition on tool electrodes and secondary discharge phenomena in micro-EDM," *Journal of Materials Processing Technology,* 212(7), pp. 1537- 1547, 2012.

[42] K. Weinert, I. Inasaki, J.W. Sutherland, T. Wakabayashi, "Dry machining and minimum quantity lubrication," *CIRP Annals - Manufacturing Technology,* 53(2), pp. 511-537, 2004.

[43] M. Kunieda, Y. Miyoshi, T. Takaya, N. Nakajima, Y. ZhanBo, M. Yoshida, "High speed 3D milling by dry EDM," *CIRP Annals - Manufacturing Technology,* 52(1), pp. 147-150, 2003.

[44] T. Saleh, M. Dahmardeh, A. Bsoul, A. Nojeh, K. Takahata, "Field-emission-assisted approach to dry micro-electro-discharge machining of carbon-nanotube forests," *J. Applied Physics,* 110 (10), pp. 103305 (1-7), 2011.

[45] W. Khalid, M.S. Mohamed Ali, M. Dahmardeh, Y. Choi, P. Yaghoobi, A. Nojeh, K. Takahata, "High-aspect-ratio, Free-form patterning of carbon nanotube forests using micro-electro-discharge machining," *Diamond and Related Materials*, 19 (11), pp. 1405-1410, 2010.

[46] C.C. Kao, J. Tao, S.W. Lee, A.J. Shih, "Dry wire electrical discharge machining of thin workpiece," *Trans. NAMRI/SME*, 34, pp. 253–260, 2006.

[47] J. Tao, A.J Shih, J. Ni, "Experimental study of the dry and near-dry electrical discharge milling processes," *Journal of Manufacturing Science and Engineering,* 130(1), pp. 011002 (1-9), 2008.

[48] D.Y. Yang, F.G. Cao, "The development of mirror machining in EDM sinking process," *Proceedings of 15th International Symposium of Electro Machining (ISEM XV), Industrial and Management Systems Engineering,* pp. 57-62, 2007.

[49] T. Tanimura, K. Isuzugawa, I. Fujita, A. Iwamoto, T. Kamitani, "Development of EDM in the mist," *Proceedings of Ninth International Symposium of Electro Machining (ISEM IX),* pp. 313-316, 1989.

[50] D.T. Pham, S.S. Dimov, S. Bigot, A. Ivanov, K. Popov, "Micro-EDM—recent developments and research issues," *Journal of Materials Processing Technology,* 149(1–3), pp. 50-57, 2004.

[51] D. Reynaerts, P. Heeren, B.H. Van, "Microstructuring of silicon by electro-discharge machining (EDM) — part I: Theory," *Sensors and Actuators A: Physical,* 60(1–3), pp. 212-218, 1997.

[52] Y. Haga, M. Esashi, "Biomedical microsystems for minimally invasive diagnosis and treatment," *Proc. IEEE,* 92(1), pp. 98-114, 2004.

[53] T. Shoa, J.D. Madden, N. Fekri, N.R. Munce, V.X.D. Yang, "Conducting polymer based active catheter for minimally invasive interventions inside arteries," *Engineering in Medicine and Biology Society, EMBS, 30th Annual International Conference of the IEEE,* pp. 2063-2066, 2008.

[54] S. Roth, *One-dimensional metals: Physics and materials science.* Newyork: Springer-Verlag, 1995.

[55] Y. B. Cohen, *Electroactive Polymer (EAP) Actuators as Artificial Muscles: Reality, Potential, and Challenges.* Second Edition, SPIE Press Monograph, vol. PM136, 2001.

[56] L. Zhang, F. Meng, Y. Chen, J. Liu, Y. Sun, T. Luo, "A novel ammonia sensor based on high density, small diameter polypyrrole nanowire arrays," *Sensors and Actuators B: Chemical,* 142(1), pp. 204-209, 2009.

[57] J. Yang, D.C. Martin, "Microporous conducting polymers on neural microelectrode arrays: I electrochemical deposition," *Sensors and Actuators B: Chemical,* 101(1–2), pp. 133-142, 2004.

[58] D. Beattie, K.H. Wong, C. Williams, L.A. Poole-Warren, T.P. Davis, C. Barner-Kowollik, "Honeycomb-structured porous films from polypyrrole-containing block copolymers prepared via RAFT polymerization as a scaffold for cell growth," *Biomacromolecules,* 7(4), pp. 1072-1082, 2006.

[59] N. Gomez, J.Y. Lee, J.D. Nickels, C.E. Schmidt, "Micropatterned polypyrrole: A combination of electrical and topographical characteristics for the stimulation of cells," *Advanced Functional Materials,* 17(10), pp. 1645-1653, 2007.

[60] L. Bay, K. West, P. Sommer-Larsen, S. Skaarup, M. Benslimane, "A conducting polymer artificial muscle with 12% linear strain," *Advanced Materials,* 15(4), pp. 310-313, 2003.

[61] P.S. Hale, P. Kappen, N., Brack, W. Prissanaroon, P.J. Pigram, J. Liesegang, "Micropatterning of fluoropolymers," *Applied Surface Science,* 252(6), pp. 2217-2228, 2006.

[62] A.N. Grace, K. Pandian, "A polypyrrole/polymethylene pattern on gold using a micro-contact printing technique," *J Solid State Electrochem,* 7(5), pp. 296-300, 2003.

[63] N.L. Jeon, I.S. Choi, B. Xu, G.M. Whitesides, "Large-area patterning by vacuum-assisted micromolding," *Advanced Materials,* 11(11), pp. 946-950, 1999.

[64] K.K.C. Lee, P.R. Herman, T. Shoa, M. Haque, J.D.W Madden, V.X.D. Yang, "Microstructuring of polypyrrole by maskless direct femtosecond laser ablation," *Advanced Materials,* 24(9), pp. 1243-1246, 2012.

[65] H.K. Tinshoff, F. Alvensleben, A. Ostendprf, G. Kamlage, S. Nolte, "Micromachining of metals using ultrashort laser pulses," *International Journal of Electrical Machining,* 4, pp. 1-6, 1999.

[66] J. Meijer, K. Du, A. Gillner, D. Hoffmann, V.S. Kovalenko, T. Masuzawa, "Laser machining by short and ultrashort pulses, state of the art and new opportunities in the age of the photons," *CIRP Annals - Manufacturing Technology,* 51(2), pp. 531-550, 2002.

[67] D.T. Pham, S.S. Dimov, P.V. Petkov, S.P. Petkov, " Laser milling," *Proceedings of the Institution of Mechanical Engineers, Part B: Journal of Engineering Manufacture,* 216(5), pp. 657-667, 2002.

[68] R.A. Serway, *Principles of physics ,* 2nd ed., Fort Worth, Texas: London: Saunders College Pub, 1998.

[69] C.J. Luis, I. Puertas, G. Villa, "Material removal rate and electrode wear study on the EDM of silicon carbide," *Journal of Materials Processing Technology,* 164–165, pp. 889-896, 2005.

[70] B. Lauwers, J.P. Kruth, K. Brans, "Development of technology and strategies for the machining of ceramic components by sinking and milling EDM," *CIRP Annals - Manufacturing Technology,* 56(1), pp. 225-228, 2007.

[71] M. Zahiruddin, M. Kunieda, "Energy distribution ratio into micro EDM electrodes," *Journal of Advanced Mechanical Design, Systems, and Manufacturing,* 4, pp. 1095-1106, 2010.

[72] E. Lassner, W. Schubert, "The element tungsten: Its properties" in *Tungsten – properties, chemistry, technology of the element, alloys, and chemical compounds*, Newyork: Kluwer Academic / Plenum Publishers, pp. 1-59, 1999.

[73] J. Fleischer, T. Masuzawa, J. Schmidt, M. Knoll, "New applications for micro-EDM," *Journal of Materials Processing Technology,* 149, pp. 246–249, 2004.

[74] M. Yamaura, T. Hagiwara, K. Iwata, "Enhancement of electrical conductivity of polypyrrole film by stretching: Counter ion effect," *Synthetic Metals,* 26(3), pp. 209-224, 1998.

[75] M. Ogasawara, K. Funahashi, T. Demura, T. Hagiwara, K. Iwata, "Enhancement of electrical conductivity of polypyrrole by stretching," *Synthetic Metals*, 14 (1-2), pp. 61 - 69, 1986.